

Concept Generalization in Visual Representation Learning

Mert Bulent Sariyildiz^{1,2} Yannis Kalantidis¹ Diane Larlus¹ Karteek Alahari²
¹NAVER LABS Europe ²Inria*

Abstract

Measuring **concept generalization**, i.e., the extent to which models trained on a set of (seen) visual concepts can be used to recognize a new set of (unseen) concepts, is a popular way of evaluating visual representations, especially when they are learned with self-supervised learning. Nonetheless, the choice of which unseen concepts to use is usually made arbitrarily, and independently from the seen concepts used to train representations, thus ignoring any semantic relationships between the two. In this paper, we argue that semantic relationships between seen and unseen concepts affect generalization performance and propose **ImageNet-CoG**, a novel benchmark on the ImageNet dataset that enables measuring concept generalization in a principled way. Our benchmark leverages expert knowledge that comes from WordNet in order to define a sequence of unseen ImageNet concept sets that are semantically more and more distant from the ImageNet-1K subset, a ubiquitous training set. This allows us to benchmark visual representations learned on ImageNet-1K out-of-the-box: we analyse a number of such models from supervised, semi-supervised and self-supervised approaches under the prism of concept generalization, and show how our benchmark is able to uncover a number of interesting insights. We will provide resources for the benchmark at <https://europe.naverlabs.com/cog-benchmark>.

1. Introduction

Supervised learning has been a key factor behind the success of deep neural network-based models for many computer vision problems. However, collecting manually-annotated large-scale data for each problem is not a sustainable paradigm. There has been an increasing effort to tackle this issue by learning *transferable* visual representations across related problems, especially to the ones where annotations are scarce. Prior work has achieved this in various ways; For instance, by imitating knowledge transfer in low-data regimes [16, 61], exploiting unlabeled data in a

*Univ. Grenoble Alpes, Inria, CNRS, Grenoble INP, LJK, 38000 Grenoble, France

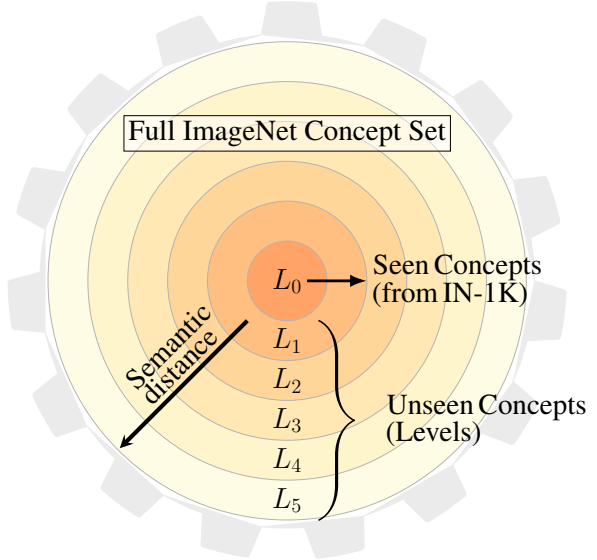


Figure 1: **ImageNet-CoG** is a new benchmark for evaluating the **Concept Generalization** capabilities of visual representations. In this benchmark, we extract features from models trained on the 1000 seen concepts of the ImageNet ILSVRC dataset [50] (IN-1K) and evaluate them on several concept generalization levels $L_1/\dots/5$, each consisting of 1000 unseen concepts sampled from the rest of ImageNet [13]. These levels are created so they contain concepts that are semantically less and less similar to IN-1K.

self- [8, 20, 23] or weakly- [28, 37, 68] supervised manner.

The quality of the learned visual representations for transfer learning is usually determined by checking whether they are useful for, i.e., *generalize* to, a wide range of downstream vision tasks. Therefore, it is important to quantify this generalization, which has several facets, such as generalization to different input distributions (e.g., from synthetic images to natural ones), to new tasks (e.g., from image classification to object detection), or to different semantic concepts (e.g., across different object categories or scene labels). Though the first two facets have received much attention recently [19, 21], we observe that a more principled analysis is needed for the last one.

As also noted by [14, 73], the effectiveness of the knowledge transfer between two tasks is closely related to the semantic similarity between the concepts of interest considered in each task. However, assessing this relatedness of tasks is not straightforward, as the semantic extent of a concept may depend on the task itself. For instance, in the case of image classification it can be a coarse- or fine-grained object category such as “car” [15] or “Russian blue” [43], as well as a less defined concept such as “dining hall” [76]. Consequently, while testing the transfer learning capabilities of models, exhaustive lists of downstream tasks have been considered to cover wide ranges of concepts [8, 30]. Yet, previous attempts discussing this issue have been limited to intuition [48, 73]. We still know little about the impact of the *semantic relationship* between the concepts seen during training visual representations and those seen during their evaluation (*seen* and *unseen* concepts, respectively).

In this paper, we propose to study the generalization capabilities of visual representations across concepts that exist in a large, popular and broad ontology, i.e., ImageNet [13], while keeping all other generalization facets fixed. Starting from a set of seen concepts, the popular ILSVRC dataset (IN-1K), we utilize semantic similarity metrics that use the hand-crafted ontology to measure semantic distance between IN-1K and every unseen concept, in order to define a sequence of five, IN-1K-sized concept generalization *levels*, each consisting of a distinct set of unseen concepts with increasing semantic distance to the seen ones. This results in a large-scale benchmark that consists of thousands of concepts, that we refer to as the **ImageNet Concept Generalization benchmark**, or **ImageNet-CoG** in short. Fig. 1 illustrates the different generalization levels.

We define a set of experiments that allows us to explore a number of important questions. (i) Which methods are more resilient to the semantic distance between seen and unseen concepts, hence generalize better? (ii) How fast can methods learn new concepts? and (iii) What makes them behave in certain ways? Defining our benchmark “around” IN-1K, allows us to fairly compare models trained on IN-1K out-of-the box. Using their publicly available pretrained models, we analyse a number of recent supervised, semi-supervised and self-supervised approaches under the prism of concept generalization, and show how our benchmark is able to uncover a number of interesting insights.

Contributions. First, we propose a systematic way of studying concept generalization, by explicitly defining a set of seen concepts which visual representation learning approaches are exposed to, and unseen concepts which are the ones visual representations need to generalize to during evaluation. Second, we design a large-scale benchmark, ImageNet-CoG, which embodies this systematic way. It builds on ImageNet and allows for a fine-grained analysis of concept generalization thanks to several increasingly more

challenging evaluation levels. Third, we analyse in depth the generalization behavior of several state-of-the-art visual representation learning approaches on our benchmark.

2. Related Work

Since our work deals with models generalizing to visual concepts beyond the training set, it is related to knowledge transfer methodologies across sets of concepts, as well as practices to evaluate the quality of visual representations.

Generalization. It typically refers to the ability of a model to perform well on new data, unavailable during its training phase. It has been studied under different perspectives such as regularization [56] and augmentation [74] techniques, links to human cognition [18], or developing quantitative metrics to better understand it, e.g., through loss functions [34] or complexity measures [42]. Several dimensions of generalization have been explored in the realm of computer vision, for instance, generalization to different visual distributions of the same concepts (domain adaptation) [11], or generalization across tasks [75]. Generalization across *concepts* is a crucial part of zero- [51, 55] and few-shot [61] learning. We also study this particular dimension, i.e., concept generalization, where the goal is to transfer knowledge acquired on a set of *seen* concepts, to newly encountered *unseen* concepts as effectively as possible.

Towards a structure of the concept space. One of the first requirements for rigorously evaluating concept generalization is structuring the concept space, in order to analyze the impact of concepts present during pretraining and transfer stages. However, previous work rarely discusses the particular choices of splits (seen vs. unseen) of their data, and random sampling of concepts remains the most common approach [22, 26, 32, 66]. A handful of methods leverage existing ontologies, for instance the WordNet graph [41] is used as a reference for splitting [12, 17, 33, 73] or domain-specific ontologies are used to test cross-domain generalization [21, 63]. These splits are however based on heuristics, instead of principled mechanisms that take into account the semantic relationship of concepts.

Transfer learning evaluations. While evaluating the quality of visual representations, it has become a standard to benchmark models on various tasks such as classification, detection, segmentation and retrieval [6, 8, 19, 23, 30, 52, 53]. These tasks are generally performed on datasets such as ImageNet-1K [50], Places [76], SUN [67], Pascal-VOC [15], MS-COCO [36]. Such choices, however, are often made *independently* from the dataset used to train the visual representations, ignoring their semantic relationship.

In summary, semantic relations between pretraining and transfer tasks has been overlooked in evaluating the quality of visual representations. To address this issue, we present a controlled evaluation protocol that factors in such relations.

3. The ImageNet Concept Generalization Benchmark

Our ImageNet-CoG is composed of multiple image sets, one for pretraining and several transfer datasets, curated in a controlled manner to measure the transfer learning performance of visual representations. Sec. 3.1 discusses our motivation for ImageNet-CoG. Sec. 3.2 presents the pretraining dataset, i.e., the set of concepts seen during the representation learning phase. Sec. 3.3 presents our approach to construct transfer datasets, i.e., sets of unseen concepts or **levels** of decreasing semantic similarity to the seen ones. Finally, Sec. 3.4 explains the proposed evaluation protocol for measuring different facets of concept generalization. We present an overview of the benchmark in the gray box.

3.1. Background

Transfer learning performance is highly sensitive to the semantic similarity between concepts in the pretraining and target datasets [14, 73]. Studying this relationship requires carefully constructed evaluation protocols controlling (i) which concepts a model has been exposed to during training (i.e., seen concepts), (ii) the semantic distance between these seen concepts and those considered for the transfer task (i.e., unseen concepts). As discussed earlier, state-of-the-art evaluation methods severely fall short on handling these aspects. We present a solution to fill in this gap by proposing ImageNet-CoG.

While designing ImageNet-CoG, we considered several important points. First, in order to exclusively focus on concept generalization, we need a controlled setup tailored for this specific aspect of generalization, i.e., we need to make sure that the only thing that changes between the pretraining and the transfer datasets is the set of concepts. In particular, we need to fix the input image distribution (i.e., natural images), and the nature of the annotation process (which may determine the statistics of images [59]).

Second, to better understand the relationship between the semantic similarity of some seen and unseen concepts and the knowledge transfer across them, we need a sufficiently broad set of concepts, not specialized fine-grained ones, such as bird species [62]. Moreover, to determine the semantic similarity between two concepts, we need an auxiliary knowledge base that can provide a notion of semantic relatedness. It can be manually defined (e.g., WordNet [41]), requiring expert knowledge, or automatically constructed, for instance by a language model (e.g., word2vec [40]).

Third, the choice of the pretraining and target datasets is crucial. We need these datasets to have diverse object-level images [3] and to be as less biased as possible, e.g., towards canonical views of concepts [39]. We also need their images to be carefully annotated for computing concept generalization precisely.

The ImageNet-CoG benchmark in a nutshell

Prerequisites:

- A set of seen concepts
- Train/val/test images associated to seen concepts
- A model pretrained on the seen concepts
- Sets of unseen concepts organized in levels $L_{1/2/3/4/5}$
- Train/val/test images for each level $L_{1/2/3/4/5}$

Phase 1: Feature Extraction

Use the model to extract image features for all image sets.

Phase 2: Evaluation

Run each experiment for seen concepts and for each level $L_{1/2/3/4/5}$, separately:

- Learn linear classifiers using all available training data
How resilient is my model to the semantic distance between seen and unseen concepts?
- Learn linear classifiers using $N \in \{1, 2, 4, \dots, 128\}$ training samples per concept.
How fast can methods adapt to new concepts?
- Apply k-means clustering on all features with $k =$ the number of concepts in each level
How does the embedding space of my model cluster for seen/unseen concepts?
- Compute the alignment and uniformity scores [64]
How is the embedding space of my model structured for seen/unseen concepts?

With all these requirements in mind, we could either collect a new dataset or build on top of an existing one. We chose the latter and narrowed our scope to the set of concepts from the full ImageNet dataset [13]. ImageNet contains 14,197,122 curated images covering 21,841 concepts, all of which are further mapped to a hand-crafted ontology [41], allowing us to define reliable semantic similarities.

3.2. Seen concepts

The first step is to select a set of concepts from ImageNet, which will be used to learn visual representations. For this, we make the obvious choice, and define seen concepts as the categories from the ubiquitous ILSVRC 2012 dataset [50] (IN-1K), which is a subset of the full ImageNet [13]. It consists of 1.28M images over 1000 concepts and has been used as the standard benchmark for evaluating novel CNN architectures (backbones) as well as self- and semi-supervised models [7, 9, 20, 23, 64, 69].

Choosing IN-1K as the seen classes further offers several advantages that make our benchmark easily applicable. (i) Practitioners would train their models on IN-1K, as this is standard practice; then they can simply evaluate on our benchmark with their pretrained models. (ii) It enables us to benchmark visual representations learned on IN-1K out-

The pool of 5754 unseen concepts from the full ImageNet (excluding IN-1K):
 (i) with at least 782 images, (ii) not in the "person" sub-tree, and (iii) leaf nodes

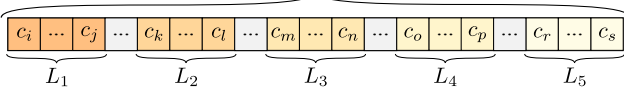


Figure 2: **Sampling of unseen concepts** for each level. We rank the 5754 eligible unseen concepts with respect to their semantic similarity to the IN-1K set using Eq. (2), and depict them ranked in this figure in decreasing similarity (from left to right). We then sample 5 groups of 1000 concepts each such that the entire range of similarities is captured. Gray-shaded areas correspond to concepts that are ignored.

-of-the box, by using the publicly available checkpoints of the models (as shown in Sec. 4).

3.3. Concept generalization levels

Our next step is defining a sequence of unseen concept sets, each with decreasing semantic similarity to the seen concepts. These datasets of unseen concepts, or *levels*, would allow to measure concept generalization in a controlled setting. Having decided on the seen dataset as IN-1K, next, we sample unseen datasets from the extended ImageNet [13] dataset, such that they are determined by their *semantic similarity* to IN-1K. We specifically use the Fall 2011 snapshot of ImageNet, that contains 21,841 concepts, including the ones in IN-1K. We perform this sampling in a controlled manner to obtain multiple unseen datasets that are increasingly less similar semantically to IN-1K. We thus create increasingly difficult transfer learning scenarios from the seen to the unseen concepts.

Design choices for concept generalization levels. We design our concept generalization levels to be as comparable as possible to IN-1K. Following [50], we select concepts with a minimum of 732 and a maximum of 1300 training images, plus 50 images for testing. As it was recently shown that a subset of ImageNet categories might exhibit problematic behavior in downstream computer vision applications [72], we make sure that no concept under the “person” sub-tree is selected. We further make sure that each level contains only leaf nodes, i.e., c_1 is not a child or parent of c_2 , for any c_1 and c_2 in any level. These requirements limit the set of eligible *unseen* ImageNet concepts from 20,841 to 5754, from which we chose 5 levels of 1000 concepts each, sampled to maximize their diversity with respect to IN-1K (details on the sampling process are presented below). This brings the total number of training images per level to 1.10 million, which is close to 1.28 million training images of IN-1K.

Semantic similarity between concepts. Computing the semantic similarity of any two concepts requires defining each concept in a semantic knowledge base. Fortunately, Im-

ageNet is built onto the word ontology of WordNet [41], where synonyms of words corresponding to distinct concepts are grouped into “synsets,” which are linked according to their semantic relationships. This further allows to utilize existing semantic similarity measures [5] that exploit the graph structure of WordNet to capture the semantic relatedness of pairs of concepts. We use the Lin similarity [35] to define concept-to-concept similarities. This similarity of two concepts c_1 and c_2 is given by:

$$\text{sim}_{\text{Lin}}(c_1, c_2) = \frac{2 \times \text{IC}(\text{LCS}(c_1, c_2))}{\text{IC}(c_1) + \text{IC}(c_2)}, \quad (1)$$

where LCS denotes the lowest common subsumer of two concepts in the WordNet graph, and $\text{IC}(c) = -\log p(c)$ is the information content of a concept with $p(c)$ being the probability of encountering an instance of the concept c in a specific corpus (in our case the subgraph of WordNet including all the seen and unseen concepts and their parents till the root node). Following [49], we define $p(c)$ as the number of concepts that exist under c .

Semantic similarity between levels. We extend the notion of concept-to-concept similarity to sets of concepts in order to define similarities between the set of seen (IN-1K) and each unseen concept. This asymmetric similarity between the set of seen concepts $\mathcal{C}_{\text{IN-1K}}$ and any unseen concept c is given by:

$$\text{sim}_{\text{IN-1K}}(c) = \max(\{\text{sim}_{\text{Lin}}(c, \tilde{c}) \mid \tilde{c} \in \mathcal{C}_{\text{IN-1K}}\}), \quad (2)$$

i.e., as the maximum similarity between *any* concept from IN-1K and c . Using Eq. (2), we rank all unseen concepts with respect to their similarity to IN-1K and sample 5 sets of 1000 concepts as shown in Fig. 2. This selection process creates challenging levels (the 1000 concepts within a level are as similar as possible to each other) which span over the full set (the margin between levels is constant and as large as possible). As a result, we maximize the range of the unseen concepts with respect to their semantic similarity to the seen ones.

Other semantic similarity measures. While designing our benchmark, we considered different semantic similarity measures before choosing Lin similarity. We explored other measures defined on the WordNet graph [38], such as the path-based Wu-Palmer [65] and the information content-based Jiang-Conrath [27]. We also considered semantic similarities based on Word2Vec representations [40] of the titles and textual descriptions of the concepts. However, our initial experiments show that benchmarks built using different similarity measures led to the same main observations we present in Sec. 4. For more details, see the supplementary material for additional results with an alternative benchmark constructed using Word2Vec.

3.4. Proposed evaluation protocol

We now present the evaluation protocol for ImageNet-CoG, and summarize the metrics we report for the different experiments presented in Sec. 4.

Feature extraction and pre-processing. We base our protocol on the assumption that *good* visual representations should generalize to new tasks with minimal effort, i.e., without fine-tuning the backbones. Therefore, for our benchmark, we only use the pretrained backbones as feature extractors and decouple representation from our evaluation. Concretely, we assume a model learnt on the training set of IN-1K; we use this model as an encoder to extract features, for IN-1K and all the five levels $L_{1/2/3/4/5}$.

Recent findings [29] suggest that residual connections prevent backbones from overfitting to pretraining tasks and the features extracted from the last layer of ResNet-like architectures generalize better to transfer tasks. In light of this, we perform all our evaluations on the features $\mathbf{x} \in \mathbb{R}^{2048}$ extracted from the global average pooling layer of the pretrained ResNet50 backbones. Moreover, in our evaluations no fine-tuning or data-augmentation is applied.

Finally, we observed that the ℓ_2 -norms of features from different models vary significantly across sets. To eliminate any bias towards the magnitudes of the features, unless otherwise stated, we ℓ_2 -normalize them.

Train/val/test splits. We randomly select 50 samples as the test set for each concept and use the remaining ones (at least 732, at most 1300) as a training set. For evaluations that involve hyperparameters, we randomly sample 20% of the training sets to choose the hyperparameters (see below). We report results only on the test sets.

Setting hyperparameters. To train linear classifiers in a fair manner for all models, we choose the learning rate and weight decay parameters on the validation sets by using Optuna [1] (for each level and IN-1K, 20% of its training set is randomly sampled as its validation set). Once we set the hyper-parameters, we train the final classifiers using the training and validation sets and compute the final performance on the test sets. We repeat the hyper-parameter selection 5 times with different seeds, and report the mean of the final scores (in most cases, standard deviation is ≤ 0.2 , and is not visible in figures).

Learning linear classifiers. We train a linear logistic regression model (LogReg) on each level. In each LogReg, we compute class logits simply as $\mathbf{s} = \mathbf{W}\mathbf{x} + \mathbf{b}$, where $\mathbf{W} \in \mathbb{R}^{1000 \times 2048}$ and $\mathbf{b} \in \mathbb{R}^{1000}$ are the parameters to learn. We use all the training samples ($N = \text{All}$) available for each concept.

Learning from few samples per concept. We also propose to evaluate data efficiency of models in learning unseen concepts, by performing few-shot concept classification on each level. We argue that this aspect of concept generalization is

Table 1: **Benchmarked models and their training data.** We use the best officially-released ResNet-50 checkpoints for each model. For **Sup**, we use the pretrained ResNet-50 model available in the torchvision package of pytorch [44]. “Add. Data” refers to the additional data used for pretraining.

Model	Abbrev.	Training data		
		IN-1K		Add. Data
		Images	Labels	
Supervised [24]	Sup	✓	✓	✗
Semi-sup. [69]	S-Sup	✓	✓	YFCC-100M
Semi-weakly-sup. [69]	S-W-Sup	✓	✓	IG-1B
MoCo-v2 [10, 23]	MoCo	✓	✗	✗
SwAV [7]	SwAV	✓	✗	✗
SimCLR-v2 [8, 9]	SimCLR	✓	✗	✗
BYOL [20]	BYOL	✓	✗	✗

particularly important as it assesses the ability of models to adapt to unseen concepts, with only a small number of annotated samples. We follow the same LogReg setup described above, except that we train LogRegs with a few samples per concept, i.e., $N \in \{1, 2, 4, 8, 16, 32, 64, 128\}$.

Clustering experiments. We perform k -Means clustering and learn 1000 cluster centroids (as many as the concepts in each level) on the training sets. We use the cuML k -Means implementation [47], repeat clustering with 3 seeds and compute cluster assignments for test samples using the centroids that gave the lowest inertia across the 3 runs. We report clustering metrics, including cluster purity and adjusted [60] and normalized mutual information scores between the cluster assignments and the labels of the test samples.

Alignment and uniformity. We compute alignment and uniformity scores, as presented in [64], using the test sets from each level and from IN-1K.

4. Evaluating state-of-the-art models

We now analyse how state-of-the-art models behave on our ImageNet-CoG, i.e., on increasingly difficult concept generalization levels. For clarity, we show in this section a subset of our experiments, which lead to the most interesting conclusions. We provide additional analyses in the **supplementary material**, together with details regarding implementation.

4.1. Models

We select a diverse set of models pretrained on IN-1K to analyse; a summary is shown in Tab. 1. We first consider three models that use the ground-truth labels of IN-1K directly. **Sup** refers to a model trained in the common supervised setting [24], while **S-Sup** and **S-W-Sup** are the semi-supervised and semi-weakly-supervised models from [69], respectively. They are pretrained on YFCC-100M [58] and IG-1B [37] and then fine-tuned on IN-1K.

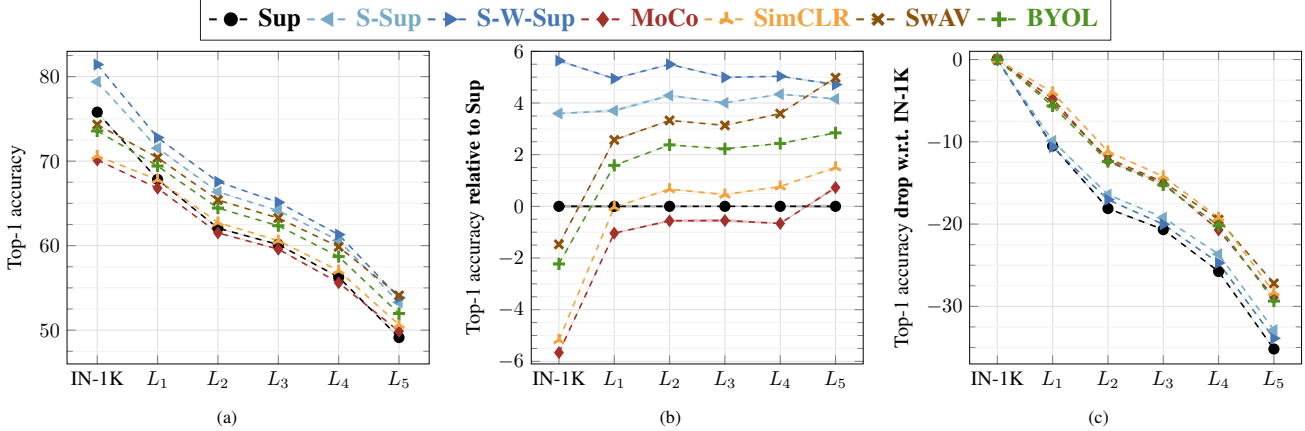


Figure 3: **Top-1 accuracy** for each method (pretrained on IN-1K) using logistic regression classifiers. We train them on pre-extracted features for the concepts in IN-1K or in one of our generalization levels ($L_{1/2/3/4/5}$), with **all** the training samples, i.e., $N = \text{All}$. (a)-(c) are visualizations of the same results from different perspectives. (a), (b) and (c) show the absolute top-1 accuracy, performance relative to **Sup**, and the drop in performance on the levels relative to IN-1K, respectively.

Finally, given the outstanding transfer learning performance that contrastive self-supervised approaches have recently exhibited, we benchmark four of the best performing ones: **BYOL** [20], **MoCo** [10, 23], **SimCLR** [8, 9] and **SwAV** [7].

MoCo and **SimCLR** share many similarities: they both train with a contrastive loss where positive pairs are obtained by applying heavy transformations to an image, with all the other images being treated as negatives. The main difference lies on the momentum encoder used by **MoCo** to sample a negative, while for **SimCLR** negatives come from the images of the same mini-batch. **BYOL** is similar to this, except that it does not require negative samples. **SwAV** is a hybrid approach which combines contrastive training with a clustering approach. It enforces consistency between the cluster assignments produced by different augmentations, and further appends a new data augmentation strategy that uses a mix of views with different resolutions. For each model, we use the best ResNet-50 [24] backbone released by their authors. As it is not clear if YFCC-100M or IG-1B contain images of our unseen concepts, these two models are not directly comparable to the others.

4.2. Generalization to unseen concepts

First, we conduct transfer learning experiments on sets of unseen concepts at different concept generalization levels. Specifically, we perform concept classification on each level separately, and study (i) how classification performance changes as we semantically move away from the seen concepts, and (ii) how fast can models adapt to unseen concepts.

Generalization using linear classifiers. We present the results in Fig. 3 and highlight the following observations.

(a) Performance of all the models (Fig. 3a) monotonically decreases as we move from levels with concepts semantically

closer to the seen ones, to those further away. This seemingly obvious observation grounds the remainder of our study.

(b) Focusing on the supervised methods, we note that the ranking $\text{S-W-Sup} > \text{S-Sup} > \text{Sup}$ remains consistent across levels. In fact, from Fig. 3b, we see that the gains of **S-W-Sup** and **S-Sup** over **Sup** remain almost constant. This shows that pretraining with additional data on IG-1B or YFCC-100M helps in generalizing better, even for semantically distant concepts. It is also noteworthy that, as we go from IN-1K to L_5 , the difference between **S-W-Sup** and **S-Sup**, despite the former utilizing an order of magnitude more data, reduces from 2% to 0.5%.

(c) Interestingly, despite the superiority of **Sup** over the self-supervised models when evaluated on IN-1K, it is outperformed by **BYOL** and **SwAV** consistently on all the unseen levels, by significant margins (see Fig. 3b). We hypothesize that by learning augmentation invariance in a soft way (**BYOL** has practically no negatives, while **SwAV** only enforces “soft” consistency through the cluster assignments of different augmentations) these two approaches produce representations that generalize better.

(d) We also note that from IN-1K to L_5 performance gaps between **Sup** and the self-supervised models progressively shift in favor of the self-supervised models. This leads to 0.8%, 5.0%, 1.5% and 2.9% margins achieved by **MoCo**, **SwAV**, **SimCLR** and **BYOL**, respectively, on L_5 (see Fig. 3b). Since these self-supervised methods essentially learn from data augmentation, it implies that learning augmentation invariances transfers better to images of unseen concepts. This is in line with the observation that data augmentation strategies can significantly boost supervised learning performance as well [74].

(e) **SwAV** degrades most gracefully. It outperforms all

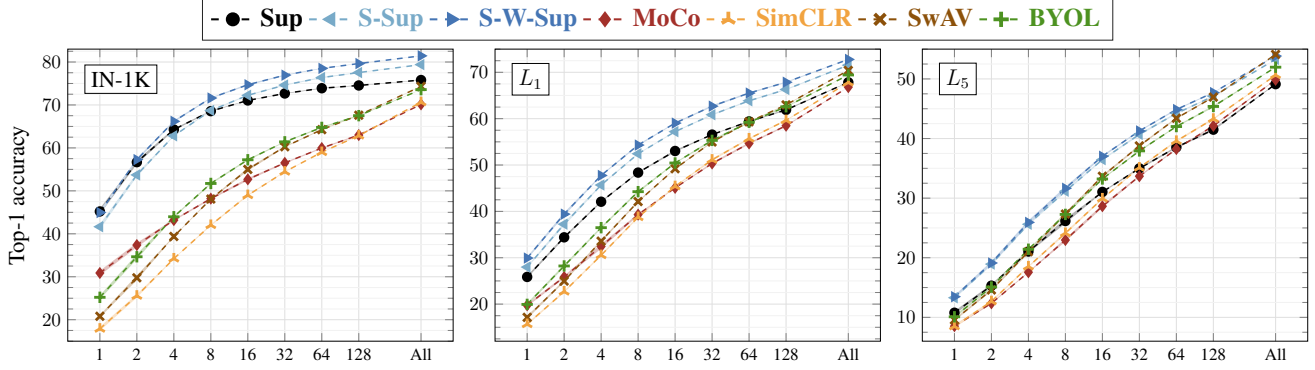


Figure 4: **Top-1 accuracy** for each method (pretrained on IN-1K) using logistic regression classifiers. We train them on pre-extracted features for the concepts in IN-1K and our generalization levels ($L_{1/2/3/4/5}$), with a **few** training samples per concept, i.e., $N = \{1, 2, 4, 8, 16, 32, 64, 128\}$. “All,” the performance when all the samples are used, is also shown for reference. From left to right: results obtained on IN-1K, L_1 , and L_5 . (See the supplementary material for the remaining levels.)

the other self-supervised approaches on all levels. Starting from L_1 , it even outperforms **Sup** by an increasing margin as the unseen concepts become semantically less similar. More surprisingly, **SwAV** outperforms **S-Sup** and **S-W-Sup** by 0.8% and 0.3% on L_5 , showing strong generalization ability. We believe that the hybrid nature of **SwAV** gives it an edge compared to other self-supervised approaches which only focus on instance discrimination, while the extra inter-scale augmentation may further provide **SwAV** with an invariance that assists generalization.

(f) Finally, from Fig. 3c we observe the difficulty in generalizing to semantically dissimilar concepts. All the methods, even **S-W-Sup** pretrained on 1 billion images, lose 25–35% of their classification power, relative to their performance on the seen classes.

Generalization from a few samples per concept. Next, we evaluate how fast each model can be trained to classify new concepts by performing few-shot image classification, and the impact of the semantic distance between unseen and seen concepts. We present these results in Fig. 4, and make the following observations.

(a) **Sup** is significantly and consistently better at learning in low-data regimes, i.e., $N = \{1, 2, 4, 8\}$, on $L_{1/2/3/4}$. However, on L_5 , the best performing self-supervised model (**BYOL** or **SwAV**) is on par or better than **Sup** for all N .

(b) As we go from IN-1K to L_5 , the amount of annotated data required for the self-supervised models to match the supervised ones decreases consistently. For instance, **SwAV** matches the performance of **Sup** when $N = 128, 64, 32, 16, 4$ on $L_{1/2/3/4/5}$, respectively.

(c) Despite the intrinsic similarity between **MoCo** and **SimCLR**, **MoCo** performs significantly better when $N = \{1, 2, 4, 8\}$ on IN-1K and L_1 . This is likely due to the memory in **MoCo** providing a diverse set of images from (possibly) all IN-1K concepts at every step during the pretraining

phase, therefore better approximating a 1-vs-all classification problem for each query. This way **MoCo** can learn better class representatives for the concepts in IN-1K and also for the ones semantically close to IN-1K.

(d) **BYOL** consistently improves over **SwAV** on IN-1K and $L_{1,2,3}$ for smaller numbers of training samples, but **SwAV** matches or outperforms **BYOL** provided enough data.

4.3. Topology of the feature space across levels

We now analyze the feature space learnt by each model in terms of clustering (Sec. 4.3.1) and pairwise-relationships (Sec. 4.3.2) of features.

4.3.1 Clustering of concepts

We expect each model, constructed with either supervised or self-supervised objectives, to learn a feature space where the images of the same concepts are (naturally) clustered. We investigate to what extent this occurs for unseen concepts.

To this end, we perform k -Means clustering and learn 1000 cluster centroids (the number of concepts in each level) on the training sets of each level. We then compute cluster purity scores between the cluster assignments and the labels of the test samples. Higher scores here imply that the features are better clustered.

Results. In Fig. 5 we plot cluster purity across levels. The results presented in this figure are consistent under different evaluation measures we explored, e.g., rand-index [46], normalized or adjusted [60] mutual information (see the supplementary material for details). We observe the following.

(a) The supervised models are significantly better than the self-supervised ones on IN-1K and all the levels. However, **BYOL** and **SwAV** reduce the gap with **Sup** on L_5 .

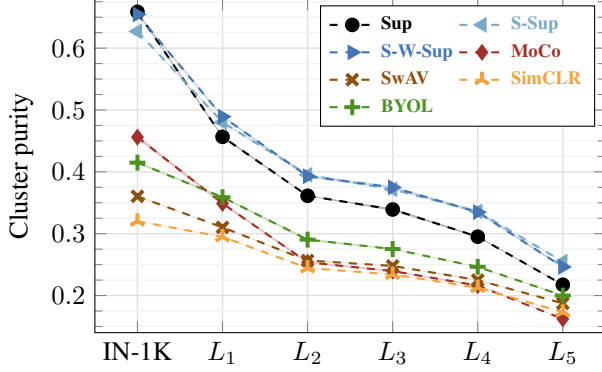


Figure 5: **Cluster purity scores** between the cluster assignments predicted by k -Means and the concept labels, computed on the test set of each level.

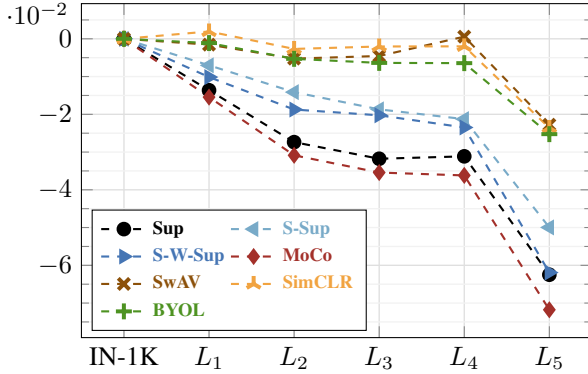


Figure 6: **Alignment over uniformity ratio** relative to IN-1K computed on the test set of each level.

(b) It is interesting that **MoCo** is the best self-supervised model on IN-1K and shares the lead with **BYOL** on L_1 .

(c) **BYOL** outperforms **SwAV** consistently on all levels. This observation seems to contradict the performance gains for **SwAV** over **BYOL** across the levels for linear classification. However, we see that the features of **BYOL** are more spread over the hyper-spheres compared to **SwAV** (see Sec. 4.3.2 and the supplementary material regarding uniformity analysis). For **BYOL**, this may suggest that although the concepts are less linearly separable, since its features are distributed more uniformly on the hyper-sphere, more natural clusters of concepts appear in its feature spaces.

4.3.2 Measuring alignment and uniformity

In our final evaluation, we visit the recently proposed alignment and uniformity measures [64], which are powerful tools to better understand the topology of a feature space. Essentially, alignment evaluates the compactness of the classes, whereas uniformity measures how spread the samples are regardless of their class label (see [64] for further details on

these scores).

Using the test sets for each level, we compute the alignment and uniformity scores separately, and for brevity, in Fig. 6 we report the ratio of alignment over uniformity scores, computed relative to IN-1K. See the supplementary material for more results.

Results. We make the following observations.

(a) For **SimCLR**, **SwAV** and **BYOL**, alignment is less affected across the levels, and the scores seem to drop slightly only on L_5 . This is an interesting observation, suggesting that for those methods the features from the same concept are as tightly connected for the seen concepts as they are for the unseen ones.

(b) The behavior noted above does not hold for the rest of the methods, i.e., **MoCo**, **Sup**, **S-Sup** and **S-W-Sup** are highly affected and result in progressively less and less “tight” concept regions from L_1 onward.

(c) In terms of uniformity (see supplementary materials for plots), we observe that **Sup** has the lowest scores ranging from (1.8 – 1.9) across all five levels and the seen classes, followed by **SwAV** ranging from (1.9 – 2.1), while all the rest of the self-supervised methods, together with the semi-supervised ones were in the (2.6 – 3.1) range across the six sets of concepts. In terms of uniformity difference relative to IN-1K, **S-W-Sup** and **MoCo** were the methods with the highest uniformity score drop on L_5 .

5. Conclusions and main observations

We introduce ImageNet-CoG, a benchmark for evaluating concept generalization, i.e., the extent to which models trained on a set of seen visual concepts can easily be adapted to recognize a new set of unseen concepts. The seen concepts in our benchmark are defined by ImageNet-1K classes, and we built the unseen ones from the full ImageNet dataset and its concept ontology. They organize in levels which are increasingly challenging in terms of concept generalization.

We present extensive evaluations of recent state-of-the-art representation learning models on ImageNet-CoG and make interesting observations: (a) self-supervised models improve their supervised counterpart on unseen concepts, and even challenge semi-supervised ones pretrained with much more data, (b) supervised models are still better at learning in extreme low-data regimes, and (c) different self-supervised methods utilize their feature spaces in different ways.

Our benchmark is designed in a way that it can be used out-of-the-box for IN-1K pretrained models, by extracting features, and performing several experiments with them, on unseen and seen concepts. We envision ImageNet-CoG to be an easy-to-use evaluation suite to study one of the most important aspects of generalization in a controlled and principled way. We plan to make the benchmark public, with extensive documentation and scripts that would enable practitioners to quickly test their models.

Acknowledgements. This work was supported in part by MIAI@Grenoble Alpes (ANR-19-P3IA-0003), and the ANR grant AVENUE (ANR-18-CE23-0011).

References

- [1] Takuya Akiba, Shotaro Sano, Toshihiko Yanase, Takeru Ohta, and Masanori Koyama. Optuna: A next-generation hyperparameter optimization framework. In *Proc. ICKDDM*, 2019. 5, 12
- [2] Philip Bachman, R Devon Hjelm, and William Buchwalter. Learning representations by maximizing mutual information across views. In *Proc. NeurIPS*, 2019. 14
- [3] T. L. Berg and A. C. Berg. Finding iconic images. In *Proc. CVPRW*, 2009. 3
- [4] James S Bergstra, Rémi Bardenet, Yoshua Bengio, and Balázs Kégl. Algorithms for hyper-parameter optimization. In *Proc. NeurIPS*, 2011. 12
- [5] Alexander Budanitsky and Graeme Hirst. Evaluating wordnet-based measures of lexical semantic relatedness. *CL*, 32(1), 2006. 4
- [6] Mathilde Caron, Piotr Bojanowski, Julien Mairal, and Armand Joulin. Unsupervised Pre-Training of Image Features on Non-Curated Data. In *Proc. ICCV*, 2019. 2
- [7] Mathilde Caron, Ishan Misra, Julien Mairal, Priya Goyal, Piotr Bojanowski, and Armand Joulin. Unsupervised learning of visual features by contrasting cluster assignments. In *Proc. NeurIPS*, 2020. 3, 5, 6
- [8] Ting Chen, Simon Kornblith, Mohammad Norouzi, and Geoffrey Hinton. A simple framework for contrastive learning of visual representations. In *Proc. ICML*, 2020. 1, 2, 5, 6, 14
- [9] Ting Chen, Simon Kornblith, Kevin Swersky, Mohammad Norouzi, and Geoffrey Hinton. Big self-supervised models are strong semi-supervised learners. In *Proc. NeurIPS*, 2020. 3, 5, 6, 14
- [10] Xinlei Chen, Haoqi Fan, Ross Girshick, and Kaiming He. Improved baselines with momentum contrastive learning. *arXiv preprint arXiv:2003.04297*, 2020. 5, 6, 14
- [11] Gabriela Csurka, editor. *Domain Adaptation in Computer Vision Applications*. Advances in Computer Vision and Pattern Recognition. Springer, 2017. 2
- [12] Jia Deng, Nan Ding, Yangqing Jia, Andrea Frome, Kevin Murphy, Samy Bengio, Yuan Li, Hartmut Neven, and Hartwig Adam. Large-scale object classification using label relation graphs. In *Proc. ECCV*, 2014. 2
- [13] J. Deng, W. Dong, R. Socher, L.-J. Li, K. Li, and L. Fei-Fei. ImageNet: A Large-Scale Hierarchical Image Database. In *Proc. CVPR*, 2009. 1, 2, 3, 4, 16
- [14] Thomas Deselaers and Vittorio Ferrari. Visual and semantic similarity in imagenet. In *Proc. CVPR*, 2011. 2, 3
- [15] M. Everingham, L. Van Gool, C. K. I. Williams, J. Winn, and A. Zisserman. The PASCAL Visual Object Classes Challenge 2007 (VOC2007) Results. 2
- [16] Chelsea Finn, Pieter Abbeel, and Sergey Levine. Model-agnostic meta-learning for fast adaptation of deep networks. In *Proc. ICML*, 2017. 1
- [17] Andrea Frome, Greg S Corrado, Jon Shlens, Samy Bengio, Jeff Dean, Marc’ Aurelio Ranzato, and Tomas Mikolov. Devise: A deep visual-semantic embedding model. In *Proc. NeurIPS*, 2013. 2
- [18] Robert Geirhos, Carlos RM Temme, Jonas Rauber, Heiko H Schütt, Matthias Bethge, and Felix A Wichmann. Generalisation in humans and deep neural networks. In *Proc. NeurIPS*, 2018. 2
- [19] Priya Goyal, Dhruv Mahajan, Abhinav Gupta, and Ishan Misra. Scaling and benchmarking self-supervised visual representation learning. In *Proc. ICCV*, 2019. 1, 2
- [20] Jean-Bastien Grill, Florian Strub, Florent Altché, Corentin Tallec, Pierre H Richemond, Elena Buchatskaya, Carl Dohersch, Bernardo Avila Pires, Zhaohan Daniel Guo, Mohammad Gheslajhi Azar, et al. Bootstrap your own latent: A new approach to self-supervised learning. In *Proc. NeurIPS*, 2020. 1, 3, 5, 6, 14
- [21] Yunhui Guo, Noel CF Codella, Leonid Karlinsky, John R Smith, Tajana Rosing, and Rogerio Feris. A new benchmark for evaluation of cross-domain few-shot learning. In *Proc. ECCV*, 2020. 1, 2
- [22] Bharath Hariharan and Ross Girshick. Low-shot visual recognition by shrinking and hallucinating features. In *Proc. ICCV*, 2017. 2
- [23] Kaiming He, Haoqi Fan, Yuxin Wu, Saining Xie, and Ross Girshick. Momentum contrast for unsupervised visual representation learning. In *Proc. CVPR*, 2020. 1, 2, 3, 5, 6
- [24] Kaiming He, Xiangyu Zhang, Shaoqing Ren, and Jian Sun. Deep residual learning for image recognition. In *Proc. CVPR*, 2016. 5, 6, 12, 18
- [25] Sergey Ioffe and Christian Szegedy. Batch normalization: Accelerating deep network training by reducing internal covariate shift. In *Proc. ICML*, 2015. 18
- [26] Dinesh Jayaraman and Kristen Grauman. Zero-shot recognition with unreliable attributes. In *Proc. NeurIPS*, 2014. 2
- [27] Jay J Jiang and David W Conrath. Semantic similarity based on corpus statistics and lexical taxonomy. *Proc. ICRCL*, 1997. 4
- [28] Armand Joulin, Laurens van der Maaten, Allan Jabri, and Nicolas Vasilache. Learning visual features from large weakly supervised data. In *Proc. ECCV*, 2016. 1
- [29] Alexander Kolesnikov, Xiaohua Zhai, and Lucas Beyer. Revisiting Self-Supervised Visual Representation Learning. In *Proc. CVPR*, 2019. 5
- [30] Simon Kornblith, Jonathon Shlens, and Quoc V. Le. Do better imagenet models transfer better? In *Proc. CVPR*, 2019. 2
- [31] Alex Krizhevsky, Ilya Sutskever, and Geoffrey E Hinton. Imagenet classification with deep convolutional neural networks. In *Proc. NeurIPS*, 2012. 12, 18
- [32] C. H. Lampert, H. Nickisch, and S. Harmeling. Learning to detect unseen object classes by between-class attribute transfer. In *Proc. CVPR*, 2009. 2
- [33] Chung-Wei Lee, Wei Fang, Chih-Kuan Yeh, and Yu-Chiang Frank Wang. Multi-label zero-shot learning with structured knowledge graphs. In *Proc. CVPR*, 2018. 2

- [34] Hao Li, Zheng Xu, Gavin Taylor, Christoph Studer, and Tom Goldstein. Visualizing the loss landscape of neural nets. In *Proc. NeurIPS*, 2018. [2](#)
- [35] Dekang Lin. An information-theoretic definition of similarity. In *Proc. ICML*, 1998. [4](#), [16](#), [17](#), [18](#)
- [36] Tsung-Yi Lin, Michael Maire, Serge Belongie, James Hays, Pietro Perona, Deva Ramanan, Piotr Dollár, and C Lawrence Zitnick. Microsoft COCO: common objects in context. In *Proc. ECCV*, 2014. [2](#)
- [37] Dhruv Mahajan, Ross Girshick, Vignesh Ramanathan, Kaiming He, Manohar Paluri, Yixuan Li, Ashwin Bharambe, and Laurens van der Maaten. Exploring the limits of weakly supervised pretraining. In *Proc. ECCV*, 2018. [1](#), [5](#)
- [38] Lingling Meng, Runqing Huang, and Junzhong Gu. A review of semantic similarity measures in wordnet. *IJHIT*, 6(1), 2013. [4](#)
- [39] Elad Meuzman and Yair Weiss. Learning about canonical views from internet image collections. In *Proc. NeurIPS*, 2012. [3](#)
- [40] Tomas Mikolov, Ilya Sutskever, Kai Chen, Greg S Corrado, and Jeff Dean. Distributed representations of words and phrases and their compositionality. In *Proc. NeurIPS*, 2013. [3](#), [4](#), [16](#)
- [41] George A Miller. Wordnet: a lexical database for english. *Commun. ACM*, 38(11), 1995. [2](#), [3](#), [4](#), [16](#), [17](#), [18](#)
- [42] Behnam Neyshabur, Srinadh Bhojanapalli, David Mcallester, and Nati Srebro. Exploring generalization in deep learning. In *Proc. NeurIPS*, 2017. [2](#)
- [43] Omkar M. Parkhi, Andrea Vedaldi, Andrew Zisserman, and C. V. Jawahar. Cats and dogs. In *Proc. CVPR*, 2012. [2](#)
- [44] Adam Paszke, Sam Gross, Francisco Massa, Adam Lerer, James Bradbury, Gregory Chanan, Trevor Killeen, Zeming Lin, Natalia Gimelshein, Luca Antiga, Alban Desmaison, Andreas Kopf, Edward Yang, Zachary DeVito, Martin Raison, Alykhan Tejani, Sasank Chilamkurthy, Benoit Steiner, Lu Fang, Junjie Bai, and Soumith Chintala. PyTorch: An imperative style, high-performance deep learning library. In *Proc. NeurIPS*. 2019. [5](#)
- [45] Fabian Pedregosa, Gaël Varoquaux, Alexandre Gramfort, Vincent Michel, Bertrand Thirion, Olivier Grisel, Mathieu Blondel, Peter Prettenhofer, Ron Weiss, Vincent Dubourg, et al. Scikit-learn: Machine learning in Python. *JMLR*, 12, 2011. [12](#), [16](#)
- [46] William M Rand. Objective criteria for the evaluation of clustering methods. *JASA*, 66(336), 1971. [7](#), [16](#)
- [47] Sebastian Raschka, Joshua Patterson, and Corey Nolet. Machine learning in python: Main developments and technology trends in data science, machine learning, and artificial intelligence. *arXiv preprint arXiv:2002.04803*, 2020. [5](#)
- [48] Mengye Ren, Eleni Triantafillou, Sachin Ravi, Jake Snell, Kevin Swersky, Joshua B Tenenbaum, Hugo Larochelle, and Richard S Zemel. Meta-learning for semi-supervised few-shot classification. In *Proc. ICLR*, 2018. [2](#)
- [49] Marcus Rohrbach, Michael Stark, and Bernt Schiele. Evaluating knowledge transfer and zero-shot learning in a large-scale setting. In *Proc. CVPR*, 2011. [4](#)
- [50] Olga Russakovsky, Jia Deng, Hao Su, Jonathan Krause, Sanjeev Satheesh, Sean Ma, Zhiheng Huang, Andrej Karpathy, Aditya Khosla, Michael Bernstein, Alexander C. Berg, and Li Fei-Fei. ImageNet Large Scale Visual Recognition Challenge. *IJCV*, 115(3), 2015. [1](#), [2](#), [3](#), [4](#), [11](#), [23](#)
- [51] Mert Bulent Sariyildiz and Ramazan Gokberk Cinbis. Gradient matching generative networks for zero-shot learning. In *Proc. CVPR*, 2019. [2](#)
- [52] Mert Bulent Sariyildiz, Julien Perez, and Diane Larlus. Learning visual representations with caption annotations. In *Proc. ECCV*, 2020. [2](#)
- [53] Ali Sharif Razavian, Hossein Azizpour, Josephine Sullivan, and Stefan Carlsson. Cnn features off-the-shelf: An astounding baseline for recognition. In *Proc. CVPRW*, 2014. [2](#)
- [54] Karen Simonyan and Andrew Zisserman. Very deep convolutional networks for large-scale image recognition. In *Proc. ICLR*, 2015. [12](#), [18](#)
- [55] Richard Socher, Milind Ganjoo, Christopher D Manning, and Andrew Ng. Zero-shot learning through cross-modal transfer. In *Proc. NeurIPS*, 2013. [2](#)
- [56] Nitish Srivastava, Geoffrey Hinton, Alex Krizhevsky, Ilya Sutskever, and Ruslan Salakhutdinov. Dropout: A simple way to prevent neural networks from overfitting. *JMLR*, 15(1), 2014. [2](#)
- [57] Christian Szegedy, Vincent Vanhoucke, Sergey Ioffe, Jon Shlens, and Zbigniew Wojna. Rethinking the inception architecture for computer vision. In *Proc. CVPR*, 2016. [12](#), [18](#)
- [58] Bart Thomee, David A Shamma, Gerald Friedland, Benjamin Elizalde, Karl Ni, Douglas Poland, Damian Borth, and Li-Jia Li. Yfcc100m: The new data in multimedia research. *Communications of the ACM*, 59(2):64–73, 2016. [5](#)
- [59] Antonio Torralba and Alexei A Efros. Unbiased look at dataset bias. In *Proc. CVPR*, 2011. [3](#)
- [60] Nguyen Xuan Vinh, Julien Epps, and James Bailey. Information theoretic measures for clusterings comparison: Variants, properties, normalization and correction for chance. *JMLR*, 11, 2010. [5](#), [7](#), [16](#)
- [61] Oriol Vinyals, Charles Blundell, Timothy Lillicrap, Daan Wierstra, et al. Matching networks for one shot learning. In *Proc. NeurIPS*, 2016. [1](#), [2](#)
- [62] C. Wah, S. Branson, P. Welinder, P. Perona, and S. Belongie. The Caltech-UCSD Birds-200-2011 Dataset. Technical Report CNS-TR-2011-001, California Institute of Technology, 2011. [3](#)
- [63] Bram Wallace and Bharath Hariharan. Extending and analyzing self-supervised learning across domains. In *Proc. ECCV*, 2020. [2](#)
- [64] Tongzhou Wang and Phillip Isola. Understanding contrastive representation learning through alignment and uniformity on the hypersphere. In *Proc. ICML*, 2020. [3](#), [5](#), [8](#), [16](#)
- [65] Zhibiao Wu and Martha Palmer. Verb semantics and lexical selection. *ACL*, 1994. [4](#)
- [66] Yongqin Xian, Christoph H Lampert, Bernt Schiele, and Zeynep Akata. Zero-shot learning—A comprehensive evaluation of the good, the bad and the ugly. *PAMI*, 41(9), 2018. [2](#)

- [67] Jianxiong Xiao, James Hays, Krista A Ehinger, Aude Oliva, and Antonio Torralba. Sun database: Large-scale scene recognition from abbey to zoo. In *Proc. CVPR*, 2010. 2
- [68] Qizhe Xie, Minh-Thang Luong, Eduard Hovy, and Quoc V. Le. Self-training with noisy student improves imagenet classification. In *Proc. CVPR*, 2020. 1
- [69] I Zeki Yalniz, Hervé Jégou, Kan Chen, Manohar Paluri, and Dhruv Mahajan. Billion-scale semi-supervised learning for image classification. *arXiv preprint arXiv:1905.00546*, 2019. 3, 5
- [70] Ikuya Yamada, Akari Asai, Jin Sakuma, Hiroyuki Shindo, Hideaki Takeda, Yoshiyasu Takefuji, and Yuji Matsumoto. Wikipedia2vec: An efficient toolkit for learning and visualizing the embeddings of words and entities from wikipedia. In *Proc. EMNLP*, 2020. 16, 17, 18
- [71] Ikuya Yamada, Hiroyuki Shindo, Hideaki Takeda, and Yoshiyasu Takefuji. Joint learning of the embedding of words and entities for named entity disambiguation. In *Proc. CONLL*, 2016. 16
- [72] Kaiyu Yang, Klint Qinami, Li Fei-Fei, Jia Deng, and Olga Russakovsky. Towards fairer datasets: Filtering and balancing the distribution of the people subtree in the imagenet hierarchy. In *Proc. FAT*, 2020. 4
- [73] Jason Yosinski, Jeff Clune, Yoshua Bengio, and Hod Lipson. How transferable are features in deep neural networks? In *Proc. NeurIPS*, 2014. 2, 3
- [74] Sangdoo Yun, Dongyoon Han, Seong Joon Oh, Sanghyuk Chun, Junsuk Choe, and Youngjoon Yoo. Cutmix: Regularization strategy to train strong classifiers with localizable features. In *Proc. ICCV*, 2019. 2, 6
- [75] Amir R. Zamir, Alexander Sax, William Shen, Leonidas J. Guibas, Jitendra Malik, and Silvio Savarese. Taskonomy: Disentangling task transfer learning. In *Proc. CVPR*, 2018. 2
- [76] Bolei Zhou, Agata Lapedriza, Aditya Khosla, Aude Oliva, and Antonio Torralba. Places: A 10 million image database for scene recognition. *PAMI*, 2017. 2

Supplementary Material

Contents

A Details on the level sizes	11
B Additional implementation details	11
B.1. Feature extraction and preprocessing	11
B.2. Training classifiers	12
C Generalization to unseen concepts...	12
C.1. ...by linear classifiers	12
C.2. ...by dimensionality reduction	12
C.3. ...by non-linear classifiers	14
D Topology of feature spaces	14
D.1. Clustering evaluation metrics	14
D.2. Alignment and uniformity scores	16
E ImageNet-CoG constructed with word2vec	16

A. Details on the level sizes

After we select 1000 concepts for each level, we make sure the image statistics are similar to the ones in IN-1K [50], i.e., we cap the number of images for each concept to a maximum of 1350 (1300 training + 50 testing), if needed. In Fig. 12 we plot the number of images per concept for each of the five levels and IN-1K.

A note on class imbalance. From Fig. 12 we see that there is minor class imbalance in all generalization levels. To investigate if imbalance had any effect on the observations of our benchmark, we further evaluated all models analyzed in Section 4 of the main paper on a variant of the benchmark where we randomly subsample the images from all selected concepts to have the same number of 732 training images, i.e., on class-balanced levels. Apart from overall reduced accuracy as a result of smaller datasets, this experiment resulted in figures almost identical to the figures shown in the main text, with all observations still holding also for the balanced case. We attribute this to the fact that class imbalance is relatively small as the minimum number of images is still high at 732 training images per class.

B. Additional implementation details

In this section, we provide additional implementation details that extend Sec. 3.4 of the main paper.

B.1. Feature extraction and preprocessing

We establish the evaluation protocols for ImageNet-CoG on top of image features extracted from pretrained CNN backbones. To extract features from a backbone we first resize an image such that its shortest side becomes S pixels, then we take a center crop of size $S \times S$ pixels. For the

AlexNet [31], VGG-16 [54] and ResNet [24] backbones $S = 224$, while for the Inception-v3 [57] backbone $S = 299$.

To be compatible with the data augmentation pipeline of the pretrained models, we adapt their normalization schemes. Concretely, we normalize each image by first dividing them by 255 (so that each pixel is in $[0, 1]$), then, except for **SimCLR**, by applying mean and std normalization to the pixels, i.e., subtracting $[0.485, 0.456, 0.406]$ from RGB channels and diving them by $[0.229, 0.224, 0.225]$, respectively.

For the AlexNet and VGG-16 backbones, we extract 4096-dimensional features from their penultimate fully-connected layers. For the ResNet and Inception-v3 backbones, we extract 2048-dimensional features from their global average pooling layers.

B.2. Training classifiers

In ImageNet-CoG, we perform 4 different types of transfer learning experiments on a particular set of concepts, i.e., IN-1K or our concept generalization levels $L_{1/2/3/4/5}$ (see Sec. 4.2 of the main paper and Sec. C): (i) Linear classification with all available data, (ii) linear classification with a few randomly selected training and all test data, (iii) linear classification over PCA-applied features with all available data and (iv) non-linear classification with all available data. In each type of experiment, we train a classifier by using the features extracted from each model, separately. Therefore, in order to evaluate each model in a fair manner in each setting, it is important to train all classifiers in the best possible way.

To train a classifier, we perform SGD with momentum=0.9 updates, using batches of size 1024, and apply weight decay regularization to parameters. We tune learning rate and weight decay hyper-parameters on a validation set randomly sampled from the training set of each concept domain (for each concept domain, 20% of the training set is randomly sampled as a validation set). We sample 30 (learning rate, weight decay) pairs using Optuna [1] with a parzen estimator [4]. After tuning the hyper-parameters, we train the final classifier on the full training set and compute its performance on the test set. We repeat this procedure 5 times with different seeds. This means that, in each repetition, we take a different random subset of the training set as a validation set and start hyper-parameter tuning with a different random pairs of hyper-parameters. Despite this stochasticity, the overall pipeline is quite robust, i.e., standard deviation in most cases is less than 0.2, therefore, is not reported in tables and not visible in figures.

Moreover, we observed that while tuning the hyper-parameters, the sample spaces for learning rate and weight decay need to be carefully selected as well. For instance, LogReg favors high learning rates, e.g., ≥ 10 , while $\text{MLP}_{\text{NoAct.}}$ tends to diverge if learning rates ≥ 0.1 , and weight decay hampers the performance of LogReg while improves MLP.

Therefore, we also supervise hyper-parameter tuning in each type of experiment by restricting the sample spaces as follows: (i) For LogReg and MLP (resp. $\text{MLP}_{\text{NoAct.}}$) we sample learning rates from $[10^{-1}, 10^2]$ (resp. $[10^{-2}, 10^1]$), (ii) for LogReg and both MLP variants we sample weight decays from $[10^{-12}, 10^{-4}]$ and $[10^{-8}, 10^{-4}]$, respectively. We will release these configurations along with our benchmark.

C. Generalization to unseen concepts...

In Sec. 4.2 of the main paper, we perform transfer learning experiments from IN-1K to our concept generalization levels $L_{1/2/3/4/5}$ using the pre-extracted image features. We do this by training linear logistic regression classifiers (LogRegs) using either all training data available for each concept (i.e., $N = \text{All}$) or only a few-annotated samples per concept (i.e., $N = \{1, 2, 4, 8, 16, 32, 64, 128\}$). In this section, we extend this analysis in two ways.

First, in Sec. C.1, we provide the *raw* top-1 accuracies obtained by LogRegs that are discussed in Sec. 4.2 of the main paper, for reference.

Second, we note that studying the transfer learning capabilities of the 2048-dimensional feature spaces learnt by different models, intact, already provides us interesting observations that we discuss in Sec. 4.2 of the main paper. These findings encourage us to further study the *compactness* of the embedding spaces (in Sec. C.2) and the *non-linear* relationship between the features and the concepts (in Sec. C.3).

C.1. ...by linear classifiers

In Tab. 2, we present the top-1 accuracies obtained by LogRegs when they are trained with all training data available for each concept (i.e., $N = \text{All}$). Note that this table presents the raw scores shown in Fig. 3 of the main paper.

In Fig. 4 of the main paper, we provide the few-shot concept classification results (i.e., when LogRegs are trained with only a few samples per concept, $N = \{1, 2, 4, 8, 16, 32, 64, 128\}$) obtained on IN-1K and on some of our generalization levels $L_{1/5}$ (results for the $L_{2/3/4}$ are not given in the main paper). In Fig. 7, we extend Fig. 4 of the main paper, and in Tab. 4 we provide the raw scores.

C.2. ...by dimensionality reduction

So far, for transfer learning, we have examined the learnt feature spaces as they are, i.e., including the variance of the features encoded in all 2048 dimensions. But, are 2048 dimensions utilized effectively in a way that they all contribute to recognizing unseen concepts?

To see this, for each model, we first reduce the dimensionality of its feature space and then train LogRegs on the compressed features for concepts in IN-1K and our generalization levels $L_{1/2/3/4/5}$. Concretely, using PCA (specifically the implementation in scikit-learn [45]), we compute

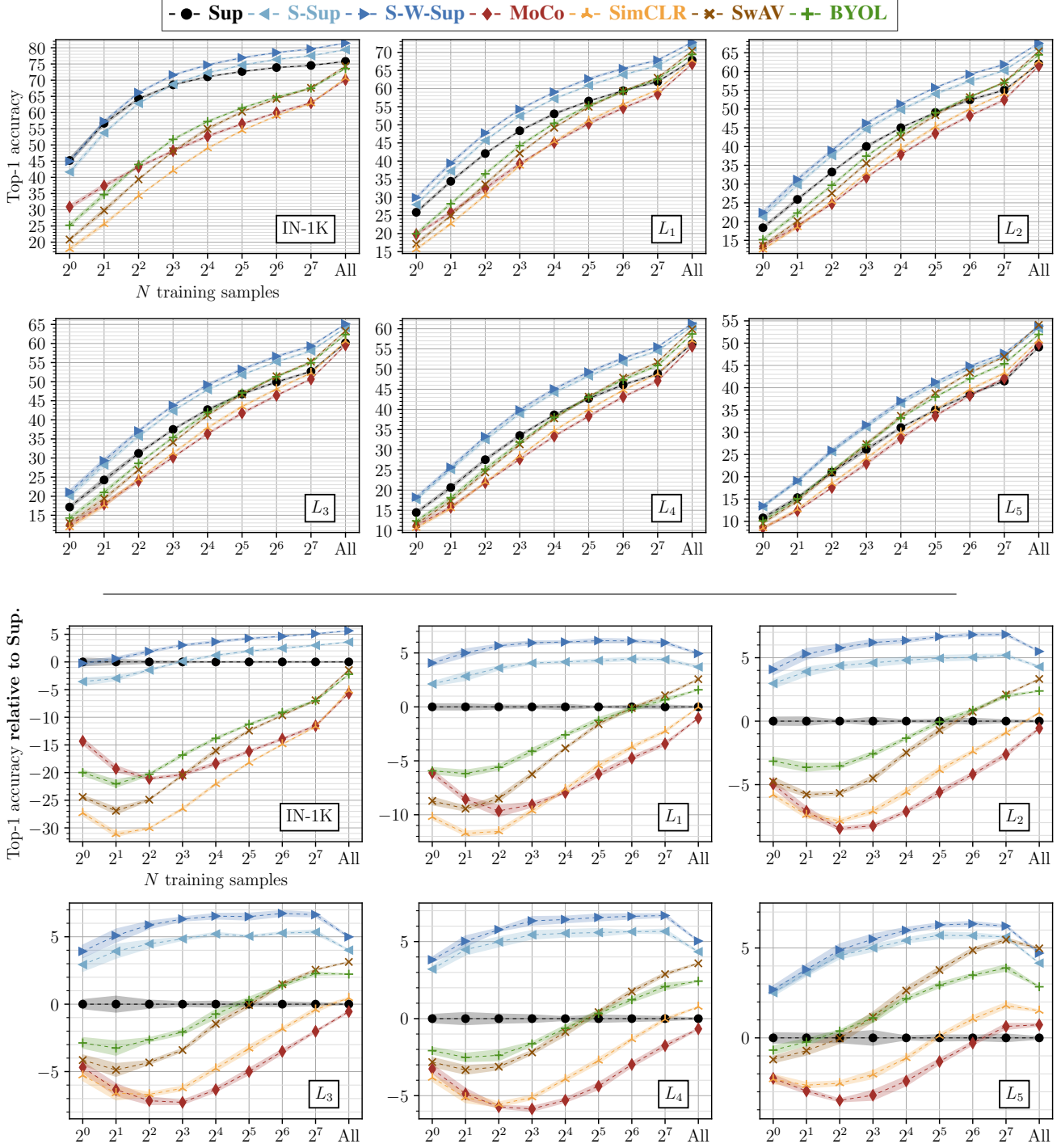


Figure 7: **(LogReg, a few training samples.)** Top-1 accuracy for each method (pretrained on IN-1K) using logistic regression classifiers. We train them on pre-extracted features for the concepts in IN-1K and our generalization levels ($L_{1/2/3/4/5}$), with a few training samples per concept, i.e., $N = \{1, 2, 4, 8, 16, 32, 64, 128\}$. “All”, the performance when all the samples are used, is also shown for reference. Top two rows; from left to right and top to bottom: results obtained on IN-1K and our concept generalization levels $L_{1/2/3/4/5}$. Bottom two rows: the same data as the top two rows, but now all accuracies are relative to Sup. This figure extends Fig. 4 in the main paper.

the first 32, 64, 128, 256, 512 and 1024 principal components from the training data available on each concept domain, and transform both the training and test sets to these principal components. Then, we follow our LogReg protocol and learn linear classifiers on each of these transformed data.

Results. We show our results in Fig. 8 (and also provide raw scores in Tab. 5), and observe the following.

(a) Interestingly, supervised classifiers do a pretty good job in learning compact spaces of visual features, which are not only useful for the seen concepts but also for the unseen concepts to some extent. For instance, on IN-1K supervised classifiers need only the first 32 principal components to achieve +63% accuracy by LogRegs. Moreover, on $L_{1/2/3/4}$, supervised classifiers can capture more discriminative patterns for the unseen concepts into the first 32 and 64 principal components compared to the self-supervised models.

(b) Surprisingly, the performance of **Sup** starts to saturate after the first 128 principal components on all concept domains, i.e., the more principal components bring diminishing improvements after the first 128 of them. Moreover, the first 1024 and 2048 principal components contribute equally to the transfer learning performance of **Sup** on all concept domains. This indicates that half of the principal components does not provide any variance for the features learned by **Sup** that is useful to discriminate the concepts.

(c) Contrarily, self-supervised models consistently improve until all the principal components are used (in log-scale), showing that the overall variance of the features are captured by more principal components.

C.3. ...by non-linear classifiers

Although linear classification has been the standard way of evaluating the transfer learning performance for pretrained models, they are limited in terms of their expressivity: they expect features extracted for the unseen concepts to be linearly separable in the high-dimensional embedding space that was learned on the seen concepts. Although this assumption holds up to some point, i.e., the models achieve +49% top-1 accuracy on L_5 (see Tab. 2), in Fig. 3.c of the main paper we can clearly see sharp relative performance drops for all models immediately starting from L_1 . Could those drops be the result of the strong linear separability assumption?

Inspired by the success of applying a non-linear projection head when learning self-supervised models [2, 8–10, 20], we further investigate what happens if we relax the linear separability requirement in our previous analysis, and learn multi-layer perceptrons (MLPs) instead.

Concretely, in this setting, we learn MLPs with 2 hidden layers each having 2048 hidden units and a ReLU non-linearity in between them. Given features $\mathbf{x} \in \mathbb{R}^{2048}$, each MLP outputs 1000-dimensional class logits $\mathbf{s} =$

$\mathbf{W}_3 \rho(\mathbf{W}_2 \rho(\mathbf{W}_1 \mathbf{x} + \mathbf{b}_1) + \mathbf{b}_2)$, where \mathbf{W}_1 and $\mathbf{W}_2 \in \mathbb{R}^{2048 \times 2048}$, \mathbf{b}_1 and $\mathbf{b}_2 \in \mathbb{R}^{2048}$ are the hidden layer parameters, $\mathbf{W}_3 \in \mathbb{R}^{1000 \times 2048}$ are the parameters of the output layer, and $\rho(\cdot)$ is the element-wise ReLU activation.

Recall that in LogRegs, we apply ℓ_2 -normalization to the features \mathbf{x} to prevent any bias towards the magnitudes of the features (we discuss this in Sec. 3.4 of the main paper). However, we argue that MLPs can adapt to the differences in the magnitudes of the features (if they need to), therefore we do not employ ℓ_2 -normalization in MLPs.

A direct performance comparison between a LogReg and its MLP counterpart is unfair: the MLP contains millions of extra learnable parameters. Therefore, we also implement $\text{MLP}_{\text{NoAct.}}$, which is the MLP with no activation function (i.e., ρ is the identity function), and compare a MLP with its $\text{MLP}_{\text{NoAct.}}$ counterpart.

Results. In Tab. 3, we show the relative performances of MLPs and $\text{MLP}_{\text{NoAct.}}$ s over their LogReg counterpart. We observe the followings.

(a) As expected, MLPs do not improve the classification performance of the supervised models on IN-1K; Because these models are already trained on IN-1K with an objective that linearly separates classes in their feature spaces. However, MLPs do improve the performance of the self-supervised models on IN-1K, i.e., 1.4%, 1.1%, 2.1% and 0.7% relative improvements over LogRegs for **MoCo**, **SwAV**, **SimCLR** and **BYOL**, respectively.

(b) Overall, the MLPs provide consistent gains for all models on our concept generalization levels $L_{1/2/3/4/5}$. Surprisingly, MLPs are most useful for semantically less similar target domains, e.g., we see significant improvements on L_4 and L_5 for all models. This supports our motivation that in the feature spaces, which are learnt on the seen classes, the semantically dissimilar unseen classes are not strictly linearly separable.

(c) The gains of MLPs are largely due to its non-linearity, i.e., ReLU activations inside. We see that $\text{MLP}_{\text{NoAct.}}$ s are on par or worse than their LogReg counterparts, except for **Sup**, for which $\text{MLP}_{\text{NoAct.}}$ s also improve significantly.

D. Topology of feature spaces

In Sec. 4.3 of the main paper, we study the topology of the learnt feature spaces for each concept domain (IN-1K and our levels $L_{1/2/3/4/5}$). We extend this analysis in the following two sub-sections (Sec. D.1, Sec. D.2).

D.1. Clustering evaluation metrics

To understand the clustering quality of the features on each concept domain, we report cluster purity scores obtained by each model in Sec. 4.3.1 of the main paper. As we explain in Sec. 3.4 of the main paper, clustering evaluation protocol consists of three steps. First, we learn cluster centroids in 2048-dimensional learnt feature spaces using the

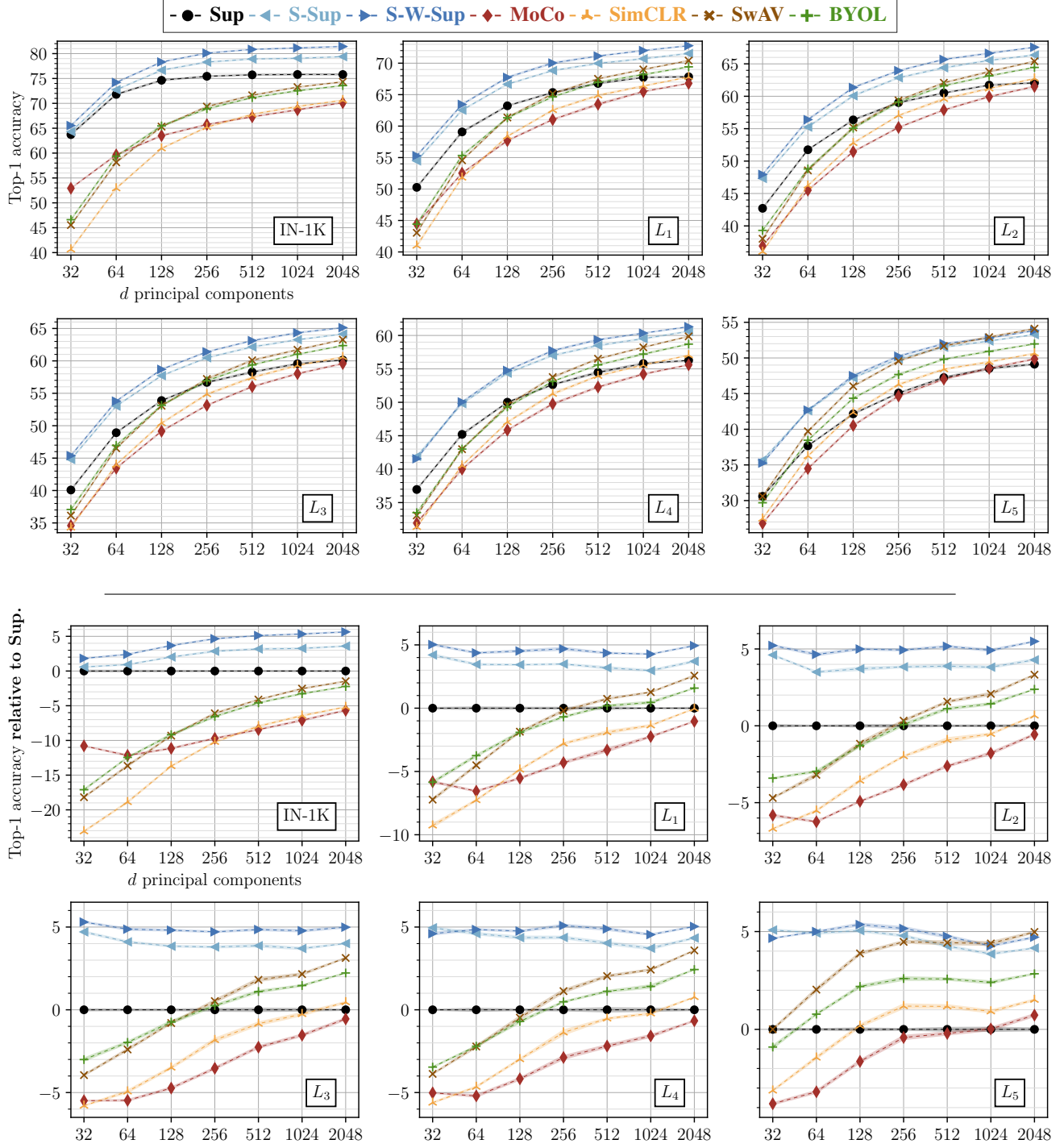


Figure 8: (PCA + LogReg, full data.) Top-1 accuracy for each method (pretrained on IN-1K) obtained by logistic regression classifiers (LogReg). First, we apply PCA to reduce the dimensionality of the pre-extracted features for the concepts in IN-1K and our generalization levels $L_{1/2/3/4/5}$. We compute the principal components using all training samples available for the concepts, i.e., $N = \text{All}$, then apply them to both training and test samples. Second, we train each LogReg on the *compressed* features. “2048”, the performance when all the principal components are used, is also shown for reference. Top two rows; from left to right and top to bottom: results obtained on IN-1K and our concept generalization levels $L_{1/2/3/4/5}$. Bottom two rows: the same data as the top two rows, but now all accuracies are relative to Sup.

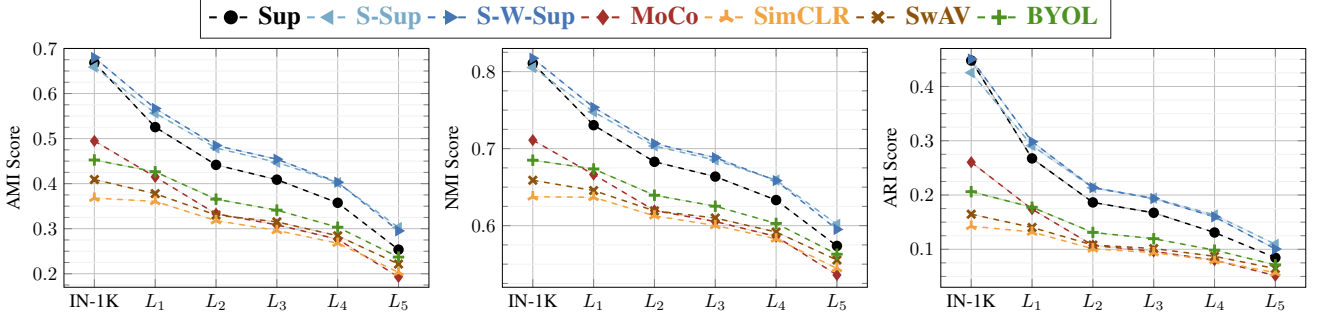


Figure 9: From left to right **adjusted mutual information** (AMI), **normalized mutual information** (NMI) and **adjusted rand-index** (ARI) scores between the cluster assignments predicted by k -Means and the concept labels, computed on the test set of each level. *Adjusted* denotes that corresponding scores are adjusted *for chance*.

training set of each concept domain, Second, we assign the corresponding test samples to the cluster centroids, Third we compute the purity scores of the test samples based on their concept labels and cluster assignments.

To compute purity scores, we first compute the *confusion matrix* \mathcal{M} between the labels and cluster assignments of the test samples such that \mathcal{M}_{ij} denotes the number of test samples belonging to concept i and assigned to cluster j . Then the purity score is computed as

$$\text{purity} = \frac{1}{1000} \sum_{i=1}^{1000} \max(\{\mathcal{M}_{ij} \mid j = \{1, \dots, 1000\}\}). \quad (3)$$

In this section, we provide additional results obtained by other popular clustering evaluation metrics, i.e., adjusted [60] and normalized mutual information, and adjusted rand-index [46] scores in Tab. 6. *Adjusted* denote that these metrics are adjusted for chance, so that random permutations result in scores close to 0. We compute these metrics using the implementations available in scikit-learn [45].

We observe that the overall behavior of the models is consistent across all of the metrics considered.

D.2. Alignment and uniformity scores

To understand the spread of the features for the unseen concepts, in Sec. 4.3.2 of the main paper, we measure their alignment and uniformity scores, both based on the pairwise relationships of the features [64]. We only provided the alignment over uniformity scores computed on our levels $L_{1/2/3/4/5}$ that are relative to IN-1K. In Fig. 10, we also report alignment and uniformity scores obtained by each model on each concept domain.

E. ImageNet-CoG constructed with word2vec

One of the requirements for studying concept generalization in a controlled manner is a knowledge base that provides the semantic relatedness of any two concepts. As

ImageNet [13] is built on the concept ontology of WordNet [41], in Sec. 3.3 of the main paper we make use of the graph structure of WordNet, and we propose a benchmark where semantic relationships are computed by the Lin measure [35].

As we mention in Sec. 3.1 of the main paper, the WordNet ontology is hand-crafted requiring expert knowledge. Therefore similarity measures that exploit this ontology (such as Lin) are arguably reliable in capturing the semantic similarity of concepts. However, it could also be desirable to learn semantic similarities automatically, for instance, using knowledge bases available online such as Wikipedia. In this section, we investigate if such knowledge bases could be used in building our ImageNet-CoG.

With this motivation, we turn our attention to semantic similarity measures that can be learned over textual data describing the ImageNet concepts. Note that each ImageNet concept is provided with a name¹ and a short description². So, the idea is to use these information to determine the semantic relatedness of any two concepts.

To do that, we consult language models to map textual data for any ImageNet concept into an embedding vector, such that semantic similarities of the concepts are absorbed in the embedding space. To achieve this, we use the skip-gram language model [40], which has been extensively used in many natural language processing tasks, to extract “word2vec” representations of all ImageNet concepts. However, we note that the name of many ImageNet concepts are *named entities* composed of multiple words, yet the vanilla skip-gram model tokenizes a textual sequence into words. To address this, we use the extension proposed by [71] that learn a skip-gram model by taking into account such named entities. More specifically, we use the skip-gram model trained on Wikipedia³ by the Wikipedia2Vec software [70].

To compute the word2vec embeddings of the ImageNet

¹<http://www.image-net.org/archive/words.txt>

²<http://www.image-net.org/archive/gloss.txt>

³April 2018 version of the English Wikipedia dump.

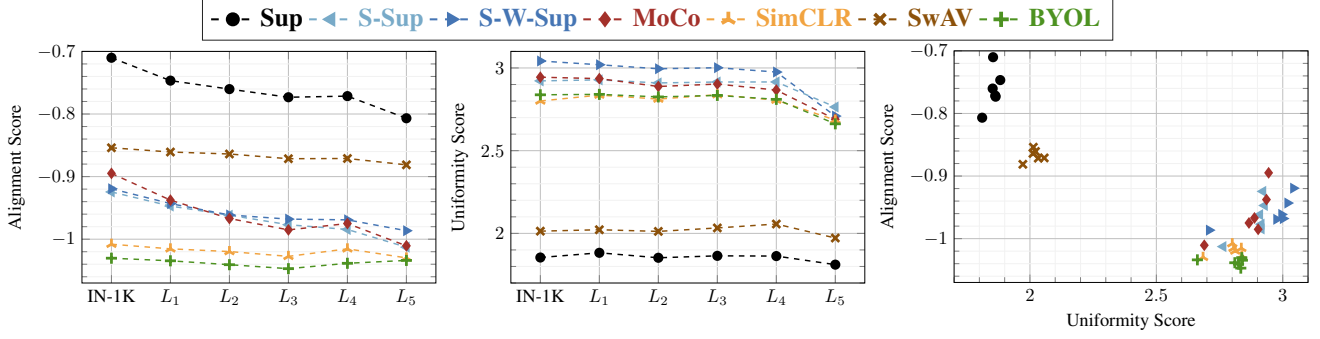


Figure 10: (left) and (middle) are **alignment** and **uniformity** scores on IN-1K and each concept generalization level $L_{1/2/3/4/5}$ separately. (right) is the scatter plot of these scores all together. All scores are computed on the test set of each level.

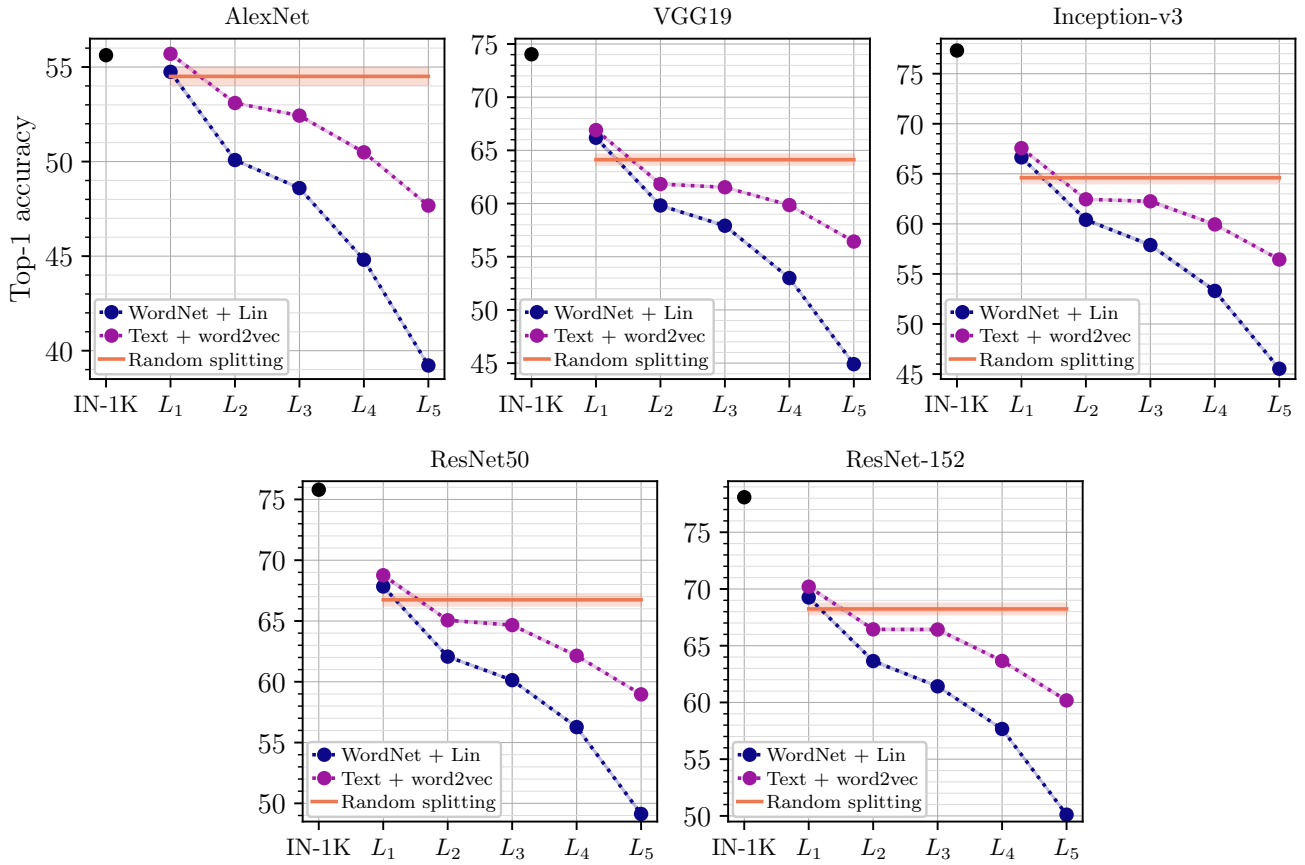


Figure 11: **Semantic similarities** of the concepts captured by (i) the Lin similarity [35] on the WordNet graph [41] and (ii) the cosine similarity of the word2vec embeddings [70], vs. **visual similarities** encoded by deep CNNs, on each concept domain (IN-1K and our generalization levels $L_{1/2/3/4/5}$). We report the performance of linear logistic regression classifiers trained on the features extracted from the penultimate layers of the CNNs. With **orange lines**, we show the transfer learning results obtained on 1000 *random* unseen concepts.

concepts, we do the followings. Firstly, we combine the names and descriptions of all concepts and learn TF-IDF weights for each unique word. Secondly, for each con-

cept, we compute two word2vec representations: the average word2vec representations of the words in its name and description, which are ultimately added up to be used

as the word2vec representation of the concept. Finally, as the semantic similarity measure, we simply use the cosine similarity between the word2vec representations of two concepts:

$$\text{sim}_{\text{w2v}}(c_1, c_2) = \frac{\omega_{c_1}^\top \omega_{c_2}}{\|\omega_{c_1}\| \cdot \|\omega_{c_2}\|}, \quad (4)$$

where ω_c denotes the word2vec representation of concept c .

Recall that in Sec. 3.3 of the main paper, first we rank the 5754 concepts in ImageNet (those having at least 782 images), w.r.t. their Lin similarity to the concepts in IN-1K. Then we sub-sample 5000 concepts to construct concept generalization levels. To create another benchmark based on the textual information of the concepts as described above, we could repeat this procedure by replacing Lin similarity with the cosine similarity we defined in Eq. (4). However, this could select a different sub-set of 5000 concepts, which, in turn, would produce two benchmarks with different sets of unseen concepts. To prevent this, we re-rank the 5000 concepts selected by the Lin similarity, based on their cosine similarity to IN-1K concepts. Then we simply divide the re-ordered concepts into 5 disjoint sequential sets.

We compare the two benchmarks constructed with different knowledge bases (i.e., the WordNet graph *vs.* textual descriptions) for some of the most popular supervised (IN-1K-pretrained) CNN architectures: AlexNet [31], VGG-16 [54] with batch-norm [25], ResNet-50/152 [24] and Inception-v3 [57] that are pretrained on the seen concepts (IN-1K) for image classification. To do that, we follow our linear logistic regression protocol that we explain in Sec. 3.3 of the main paper. Concretely, first we extract image features from the penultimate layers of the CNNs (the ones before the last fully-connected layers producing 1000-dimensional class logits), then we train LogRegs on each concept domain separately.

We report the results in Fig. 11 for the two benchmarks as well as for randomly selected 1000 concept subsets. We see that the benchmark constructed by WordNet ontology [41] and Lin similarity [35] yields much more challenging concept generalization levels compared to the one obtained by using textual data and a skip-gram language model [70] pretrained on Wikipedia. This is especially visible when comparing the LogReg performance on the levels $L_{3/4/5}$ produced by each technique. We argue that this could be due to the fact that WordNet is an ontology hand-crafted by experts and is able to better approximate the semantic similarity of two concepts compared to the machine-learning based skip-gram model. We see that for a given level L_i WordNet + Lin manages to gather together the concepts that are harder to discriminate and the resulting LogReg performance is lower. This experiment, however, shows that it is possible to create a similar benchmark using automatic semantic similarity scores, something that could be the only way in the absence of hand-crafted ontologies.

Table 2: **(LogReg, full training set.)** Top-1 accuracy for each method (pretrained on IN-1K) obtained by logistic regression classifiers (LogReg). We train each LogReg on the pre-extracted features for the concepts in a particular concept domain (i.e., IN-1K or one of our generalization levels $L_{1/2/3/4/5}$), using **all training samples** available for the concepts, i.e., $N = \text{All}$. **This is a table view of Fig. 3 in the main paper.**

Model	Concept Domain					
	IN-1K	L_1	L_2	L_3	L_4	L_5
Sup	75.8	67.8	62.1	60.1	56.3	49.1
S-Sup	79.4	71.5	66.4	64.1	60.6	53.3
S-W-Sup	81.4	72.8	67.6	65.1	61.3	53.8
MoCo	70.1	66.8	61.5	59.6	55.6	49.9
SwAV	74.3	70.4	65.4	63.3	59.9	54.1
SimCLR	70.6	67.8	62.7	60.6	57.0	50.6
BYOL	73.6	69.4	64.4	62.4	58.7	52.0

Table 3: **Logistic regression classifiers (LogReg) vs. multi-layer perceptrons** with (MLP) and without ($\text{MLP}_{\text{NoAct.}}$) activation functions. MLP is a standard multi-layer perceptron with ReLU activations after its hidden layers, whereas $\text{MLP}_{\text{NoAct.}}$ has no non-linearity inside, i.e., each activation function is the identity function. For LogRegs we report their absolute top-1 scores (also available in Tab. 2). For MLPs and $\text{MLP}_{\text{NoAct.}}$ s we report relative scores w.r.t corresponding LogRegs in percentages, i.e., $100 \times \frac{\text{MLP} - \text{LogReg}}{\text{LogReg}}$.

Model	Classifier	IN-1K	L_1	L_2	L_3	L_4	L_5
Sup	LogReg	75.8	67.8	62.1	60.1	56.3	49.1
Sup	$\text{MLP}_{\text{NoAct.}}(2)$	−0.2%	+0.5%	+0.8%	+0.3%	+0.9%	+1.8%
Sup	MLP(2)	−0.2%	+1.1%	+1.5%	+1.6%	+2.1%	+4.7%
S-Sup	LogReg	79.4	71.5	66.4	64.1	60.6	53.3
S-Sup	$\text{MLP}_{\text{NoAct.}}(2)$	−0.8%	−0.2%	+0.1%	+0.1%	−0.2%	+0.7%
S-Sup	MLP(2)	−0.0%	+1.3%	+2.1%	+2.3%	+2.8%	+5.2%
S-W-Sup	LogReg	81.4	72.8	67.6	65.1	61.3	53.8
S-W-Sup	$\text{MLP}_{\text{NoAct.}}(2)$	−0.9%	−0.2%	−0.0%	+0.2%	−0.0%	+0.6%
S-W-Sup	MLP(2)	−0.2%	+1.2%	+1.8%	+2.2%	+2.7%	+5.0%
MoCo	LogReg	70.1	66.8	61.5	59.6	55.6	49.9
MoCo	$\text{MLP}_{\text{NoAct.}}(2)$	−0.0%	−0.6%	−0.6%	−0.7%	−0.4%	+0.3%
MoCo	MLP(2)	+1.4%	+1.0%	+1.5%	+0.5%	+2.2%	+3.9%
SwAV	LogReg	74.3	70.4	65.4	63.3	59.9	54.1
SwAV	$\text{MLP}_{\text{NoAct.}}(2)$	+0.1%	−0.4%	−0.5%	−0.6%	−0.3%	+0.3%
SwAV	MLP(2)	+1.1%	+1.3%	+1.8%	+2.0%	+2.5%	+4.7%
SimCLR	LogReg	70.6	67.8	62.7	60.6	57.0	50.6
SimCLR	$\text{MLP}_{\text{NoAct.}}(2)$	+0.0%	−0.3%	−0.4%	−0.3%	−0.4%	+0.4%
SimCLR	MLP(2)	+2.1%	+2.2%	+3.0%	+3.4%	+4.1%	+6.9%
BYOL	LogReg	73.6	69.4	64.4	62.4	58.7	52.0
BYOL	$\text{MLP}_{\text{NoAct.}}(2)$	−0.2%	−0.4%	−0.4%	−0.8%	−0.6%	+0.2%
BYOL	MLP(2)	+0.7%	+1.3%	+1.8%	+1.7%	+2.2%	+5.4%

Table 4: (**LogReg, a few training samples.**) A table view of Fig. 7.

Model	Concept Domain	Number of Training Samples (N)								
		1	2	4	8	16	32	64	128	All
Sup	IN-1K	45.2	56.7	64.3	68.6	71.0	72.7	73.9	74.5	75.8
S-Sup	IN-1K	41.7	53.7	62.8	68.7	72.2	74.6	76.4	77.5	79.4
S-W-Sup	IN-1K	45.0	57.3	66.2	71.6	74.7	76.9	78.5	79.6	81.4
MoCo	IN-1K	30.9	37.4	43.2	48.2	52.7	56.5	60.0	63.0	70.1
SwAV	IN-1K	20.8	29.8	39.4	48.1	55.0	60.3	64.3	67.6	74.3
SimCLR	IN-1K	17.9	25.6	34.2	42.0	49.0	54.4	59.0	62.9	70.6
BYOL	IN-1K	25.2	34.7	44.0	51.7	57.2	61.4	64.8	67.5	73.6
Sup	L_1	25.9	34.4	42.1	48.4	53.0	56.6	59.4	61.9	67.8
S-Sup	L_1	28.0	37.2	45.7	52.4	57.2	60.9	63.9	66.3	71.5
S-W-Sup	L_1	29.9	39.4	47.7	54.3	59.0	62.7	65.5	67.9	72.8
MoCo	L_1	19.7	25.8	32.4	39.3	45.1	50.3	54.7	58.5	66.8
SwAV	L_1	17.1	25.0	33.6	42.1	49.2	55.0	59.3	63.0	70.4
SimCLR	L_1	15.7	22.7	30.5	38.7	45.4	51.1	55.7	59.7	67.8
BYOL	L_1	19.9	28.2	36.5	44.3	50.4	55.3	59.2	62.6	69.4
Sup	L_2	18.4	25.9	33.2	40.0	45.0	49.1	52.4	55.1	62.1
S-Sup	L_2	21.3	29.8	37.6	44.6	49.8	54.0	57.5	60.3	66.4
S-W-Sup	L_2	22.4	31.2	39.0	46.2	51.4	55.7	59.3	61.9	67.6
MoCo	L_2	13.4	18.8	24.8	31.8	37.9	43.5	48.2	52.4	61.5
SwAV	L_2	13.6	20.1	27.5	35.5	42.6	48.4	53.2	57.2	65.4
SimCLR	L_2	12.6	18.5	25.4	32.9	39.4	45.2	50.0	54.2	62.7
BYOL	L_2	15.2	22.3	29.7	37.5	43.7	49.0	53.3	57.0	64.4
Sup	L_3	17.2	24.2	31.2	37.5	42.7	46.8	49.9	52.7	60.1
S-Sup	L_3	20.1	28.2	35.7	42.3	47.9	51.8	55.2	58.0	64.1
S-W-Sup	L_3	21.1	29.3	37.1	43.8	49.2	53.3	56.6	59.3	65.1
MoCo	L_3	12.5	17.9	24.1	30.2	36.3	41.8	46.4	50.7	59.6
SwAV	L_3	13.0	19.4	26.9	34.1	41.2	46.7	51.4	55.2	63.3
SimCLR	L_3	11.9	17.6	24.5	31.2	37.9	43.5	48.1	52.3	60.6
BYOL	L_3	14.3	21.0	28.6	35.4	41.9	47.1	51.3	54.9	62.4
Sup	L_4	14.5	20.6	27.5	33.5	38.7	42.7	46.1	48.8	56.3
S-Sup	L_4	17.7	25.1	32.5	39.0	44.2	48.3	51.7	54.5	60.6
S-W-Sup	L_4	18.3	25.7	33.3	39.9	45.1	49.3	52.7	55.5	61.3
MoCo	L_4	11.2	15.8	21.8	27.7	33.4	38.3	43.1	47.1	55.6
SwAV	L_4	11.6	17.3	24.4	31.3	37.8	43.1	47.9	51.7	59.9
SimCLR	L_4	10.6	15.5	22.0	28.4	34.7	40.0	44.8	48.8	57.0
BYOL	L_4	12.4	18.1	25.2	31.9	38.0	43.0	47.3	50.9	58.7
Sup	L_5	10.8	15.3	21.0	26.2	31.0	35.0	38.5	41.5	49.1
S-Sup	L_5	13.3	18.9	25.6	31.2	36.5	40.7	44.2	47.1	53.3
S-W-Sup	L_5	13.5	19.1	25.9	31.7	37.0	41.3	44.9	47.7	53.8
MoCo	L_5	8.5	12.4	17.6	23.0	28.6	33.7	38.2	42.1	49.9
SwAV	L_5	9.6	14.6	21.0	27.3	33.7	38.8	43.4	47.0	54.1
SimCLR	L_5	8.5	12.7	18.5	24.1	29.9	35.1	39.6	43.3	50.6
BYOL	L_5	10.1	15.1	21.4	27.3	33.2	37.9	42.0	45.4	52.0

Table 5: (PCA + LogReg, full data.) A table view of Fig. 8.

Model	Concept Domain	Number of Principal Components (d)						
		32	64	128	256	512	1024	2048
Sup	IN-1K	63.7	71.8	74.6	75.4	75.7	75.8	75.8
S-Sup	IN-1K	64.3	72.7	76.7	78.3	78.9	79.1	79.4
S-W-Sup	IN-1K	65.5	74.2	78.3	80.1	80.8	81.1	81.4
MoCo	IN-1K	52.9	59.6	63.5	65.7	67.3	68.7	70.1
SwAV	IN-1K	45.5	58.2	65.3	69.3	71.6	73.3	74.3
SimCLR	IN-1K	40.6	52.9	60.9	65.2	67.8	69.4	70.6
BYOL	IN-1K	46.6	59.4	65.5	68.9	71.2	72.5	73.6
Sup	L_1	50.3	59.1	63.2	65.3	66.8	67.7	67.8
S-Sup	L_1	54.5	62.5	66.7	68.8	70.0	70.7	71.5
S-W-Sup	L_1	55.3	63.4	67.7	70.0	71.1	72.0	72.8
MoCo	L_1	44.5	52.5	57.7	61.0	63.5	65.5	66.8
SwAV	L_1	43.0	54.6	61.4	65.1	67.5	69.0	70.4
SimCLR	L_1	41.0	51.8	58.4	62.5	64.9	66.4	67.8
BYOL	L_1	44.4	55.3	61.3	64.7	67.0	68.2	69.4
Sup	L_2	42.7	51.8	56.4	59.0	60.5	61.7	62.1
S-Sup	L_2	47.3	55.2	60.1	62.9	64.4	65.5	66.4
S-W-Sup	L_2	47.9	56.4	61.4	64.0	65.7	66.6	67.6
MoCo	L_2	36.9	45.5	51.4	55.2	57.9	59.9	61.5
SwAV	L_2	38.0	48.6	55.2	59.4	62.1	63.8	65.4
SimCLR	L_2	36.0	46.2	52.8	57.0	59.6	61.2	62.7
BYOL	L_2	39.3	48.8	55.1	59.1	61.6	63.1	64.4
Sup	L_3	40.1	48.9	53.9	56.7	58.3	59.6	60.1
S-Sup	L_3	44.8	53.0	57.7	60.5	62.1	63.3	64.1
S-W-Sup	L_3	45.4	53.8	58.7	61.4	63.1	64.3	65.1
MoCo	L_3	34.6	43.4	49.1	53.1	56.0	58.0	59.6
SwAV	L_3	36.1	46.5	53.1	57.2	60.1	61.7	63.3
SimCLR	L_3	34.3	44.0	50.4	54.9	57.4	59.3	60.6
BYOL	L_3	37.1	47.0	53.1	56.9	59.4	61.0	62.4
Sup	L_4	37.0	45.2	50.0	52.6	54.5	55.8	56.3
S-Sup	L_4	41.9	49.8	54.4	57.0	58.5	59.5	60.6
S-W-Sup	L_4	41.6	50.1	54.8	57.7	59.4	60.3	61.3
MoCo	L_4	31.9	40.0	45.8	49.8	52.3	54.2	55.6
SwAV	L_4	33.1	43.0	49.5	53.8	56.5	58.2	59.9
SimCLR	L_4	31.3	40.5	47.0	51.3	53.9	55.6	57.0
BYOL	L_4	33.5	43.0	49.3	53.1	55.6	57.2	58.7
Sup	L_5	30.6	37.7	42.2	45.1	47.2	48.5	49.1
S-Sup	L_5	35.7	42.6	47.2	49.9	51.5	52.4	53.3
S-W-Sup	L_5	35.3	42.7	47.5	50.2	52.0	52.8	53.8
MoCo	L_5	26.8	34.5	40.5	44.7	47.0	48.5	49.9
SwAV	L_5	30.6	39.7	46.0	49.6	51.7	52.9	54.1
SimCLR	L_5	27.5	36.2	42.3	46.3	48.4	49.4	50.6
BYOL	L_5	29.7	38.5	44.4	47.7	49.8	50.9	52.0

Table 6: **Clustering evaluation measures.** A table view of Fig. 9 and Fig. 5 of the main paper.

Model	Concept Domain					
	IN-1K	L_1	L_2	L_3	L_4	L_5
<i>Cluster Purity Scores</i>						
Sup	0.659	0.457	0.361	0.339	0.295	0.217
S-Sup	0.627	0.480	0.395	0.372	0.336	0.255
S-W-Sup	0.654	0.489	0.393	0.375	0.335	0.246
MoCo	0.456	0.349	0.254	0.240	0.216	0.162
SwAV	0.360	0.310	0.257	0.248	0.225	0.187
SimCLR	0.320	0.295	0.244	0.234	0.213	0.173
BYOL	0.415	0.359	0.290	0.275	0.246	0.200
<i>AMI Scores</i>						
Sup	0.668	0.525	0.442	0.409	0.357	0.254
S-Sup	0.659	0.557	0.479	0.447	0.402	0.303
S-W-Sup	0.680	0.567	0.485	0.454	0.403	0.295
MoCo	0.495	0.415	0.333	0.309	0.277	0.193
SwAV	0.409	0.378	0.330	0.315	0.284	0.222
SimCLR	0.368	0.361	0.318	0.296	0.268	0.203
BYOL	0.453	0.426	0.366	0.341	0.303	0.237
<i>NMI Scores</i>						
Sup	0.811	0.730	0.683	0.664	0.633	0.574
S-Sup	0.805	0.748	0.703	0.685	0.659	0.602
S-W-Sup	0.817	0.754	0.707	0.688	0.658	0.595
MoCo	0.711	0.666	0.620	0.605	0.586	0.536
SwAV	0.659	0.646	0.619	0.610	0.592	0.555
SimCLR	0.637	0.637	0.613	0.600	0.583	0.544
BYOL	0.685	0.674	0.639	0.625	0.603	0.563
<i>ARI Scores</i>						
Sup	0.448	0.267	0.186	0.167	0.131	0.084
S-Sup	0.425	0.291	0.213	0.194	0.163	0.109
S-W-Sup	0.450	0.298	0.214	0.193	0.160	0.101
MoCo	0.260	0.174	0.107	0.096	0.080	0.051
SwAV	0.165	0.140	0.108	0.101	0.087	0.064
SimCLR	0.143	0.132	0.101	0.094	0.079	0.057
BYOL	0.206	0.177	0.131	0.119	0.098	0.071

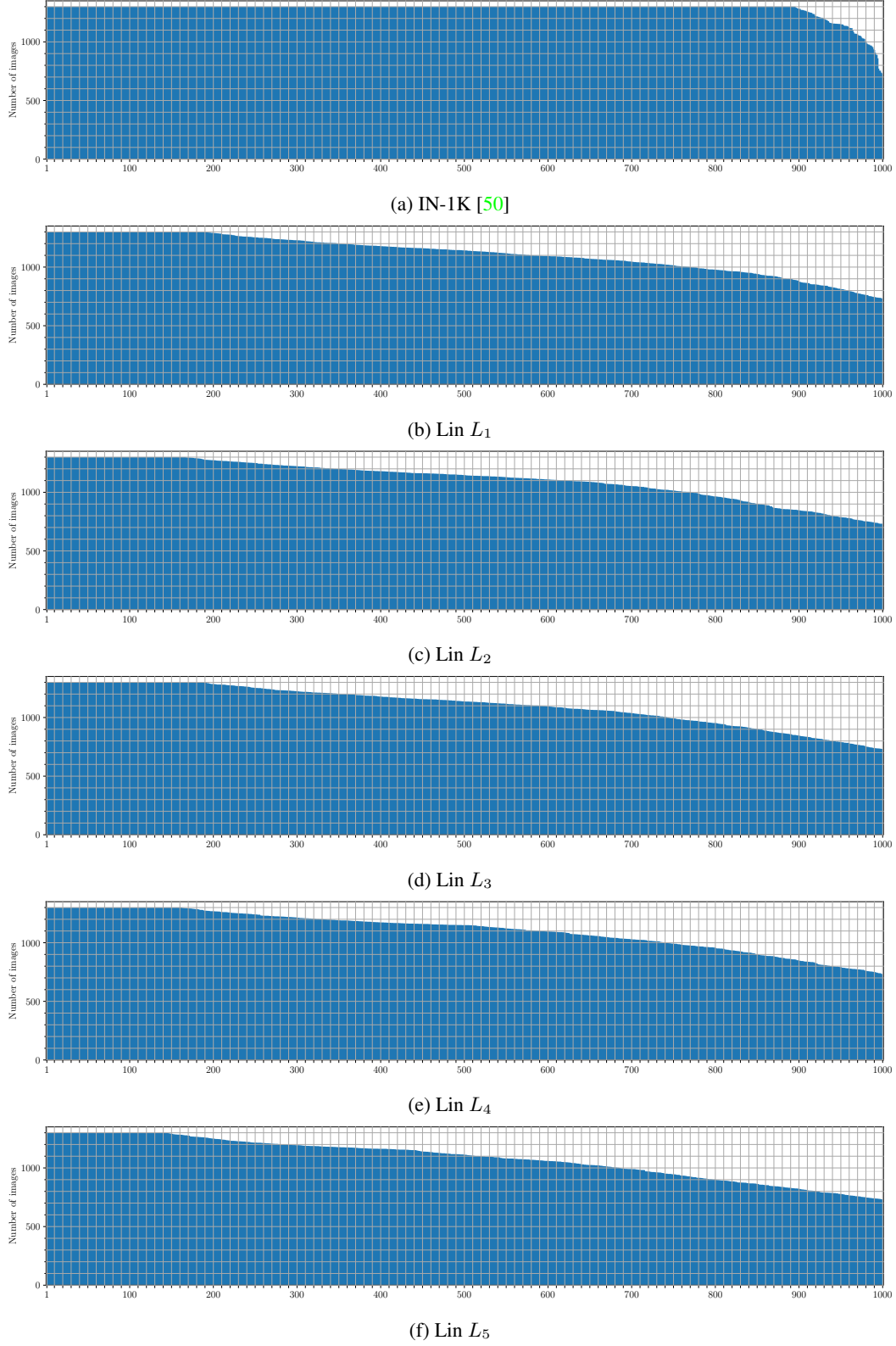


Figure 12: The number of images for IN-1K [50] and each of the concept generalization levels obtained by Lin similarity($L_1/\dots/5$). We end up with 1,166,497, 1,162,532, 1,157,993, 1,156,172 and 1,131,387 images in total for levels $L_1/2/3/4/5$ respectively.